INDIRECT CONSEQUENCES OF NUCLEAR INCIDENTS/ACCIDENTS

INDIRECT CONSEQUENCES OF EXPOSURE TO RADIATION IN DOSES RELEVANT TO NUCLEAR INCIDENTS AND ACCIDENTS

By CHANDULA FERNANDO, B.Sc.

A Thesis Submitted to the School of Graduate Studies in Partial Fulfilment of the Requirements for the Degree Master of Science

McMaster University MASTER OF SCIENCE (2018) Hamilton, Ontario

(Radiation Science – Radiation Biology)

TITLE:	Indirect Consequences of Exposure to Radiation in Doses Relevant to Nuclear Incidents and Accidents
AUTHOR:	Chandula Fernando B.Sc. (McMaster University)
SUPERVISOR:	Professor Carmel E. Mothersill
NUMBER OF PAGES:	lxxxviii, 88

ABSTRACT

At low doses, relevant to nuclear incidents and accidental releases of radioactivity, the detriment of radiation extends beyond direct effects. This thesis investigates genomic instability, a subclass of non-targeted effects where damage and lethality is transmitted vertically and expressed in the progeny of cells many generations after initial radiation exposure. Through a series of experiments using clonogenic assay of human and fish cell culture, studies described in this thesis describe lethal mutations, hyper radiosensitivity and increased radioresistance – processes involving repair mechanisms that dictate survival in cells exposed to low doses. Further study investigates the difference in the relative biological effect of alpha particle radiation compared to what is expected at high doses. Results demonstrate increased radioresistance in a human cell line while also revealing increased lethality in a fish cell line confirming the need for consideration of dose-dependence as well as variance in behaviors of different cell lines and species. It is hoped the conclusions of this thesis will inspire the creation of protocols with greater attention to the indirect consequences of exposure to radiation at doses relevant to nuclear incidents and accidents.

ACKNOWLEDGEMENTS

I am especially grateful to Dr. Carmel Mothersill for sharing her immense patience and guidance over the past two years. My academic career will forever be inspired by her insights and dedication to the field. I extend my thanks to my committee members Dr. John Eyles and Dr. Niko Yiannakoulias for their invaluable feedback and support. I would like to thank Dr. Soo Hyun Byun for his vital help in creating the Monte Carlo simulations. I am indebted to my lab members, particularly Dr. Nguyen (Nathan) Vo, Dr. Xiaopei Shi, Dusan Vukmirovic and Jason Cohen without whom I would be lost. Finally, I would like to thank my family and especially Katie for your continued support and encouragement over the years.

TABLE OF CONTENTS

Abstract ..... *iii*

Acknowledgements ..... *iv*

Table of Contents ..... *v*

List of Figures ..... *vii*

List of Tables ..... *x*

Introduction 1

1.1 Motivation *1*

1.2 Background *2*

1.3 Purpose *7*

1.4 Cell culture *9*

1.5 Experimental Setup *11*

Lethal mutations in a human glioma cell line with metastatic potential 14

2.1 Cell culture *16*

2.2 Acute irradiation using a Cs-137 source *16*

2.3 Quantitative methods *17*

2.4 Results *18*

2.5 Discussion *21*

Relative biological effect of alpha particle radiation on low dose phenomena 23

3.1 Cell culture *24*

3.2 Chronic irradiation using Ra-226 in medium 25

3.3 Acute irradiation using a Cs-137 source 27

3.4 Determining γ dose from Ra-226 28

3.5 Curve modelling 30

3.6 Results 31

3.7 Discussion 41

Conclusions and Future Directions 45

4.1 Direct effects 45

4.2 Cell culture 50

4.3 Further indirect consequences 57

References 65

LIST OF FIGURES

Figure 1 – Following staining using diluted Fuchsin-Carbol, colonies with more than 50 cells are distinctly visible allowing for counting without the use of a microscope 10

Figure 2 – Diagram describing the general experimental setup for lethal mutation experiments. Flasks marked with 'R' (blue) are reporter flasks while flasks marked with 'P' (black) are donor flasks. Only cells in the initial passage receive direct irradiation. The above is replicated for each dose observed 13

Figure 3 – One iteration of the Monte Carlo simulation determining the spatial distribution of Ra-226 particles emitting gamma energy per emission (500 mBq/ml shown). The gamma energy is shown in MeV according to the legend 29

Figure 4 – Residual survival fractions as represented through fitted curves following the induced-repair model. Green curves represent cells exposed to Cs-137 and their progeny while black curves represent cells exposed to Ra-226 and their progeny. The darkest/solid curves represent the initial survival of the progenitors directly receiving radiation, medium/dashed curves represent the first observation of progeny (not directly irradiated), and the lightest/dotted curves represent the second observation of progeny (not directly irradiated). There were roughly 7 days between observations (time taken to reach 80-90% confluency) 33

Figure 5 – Calculated relative effect of alpha particle exposure on residual survival of HaCaT cells, as a function of effective gamma dose to progenitor cells. The darkest/solid curve represents the initial survival of progenitors directly receiving radiation, the medium/dashed curve represents the first observation of progeny (not directly irradiated), and the lightest/dotted curve represents the

second observation of progeny (not directly irradiated). There were roughly 7 days between observations (time taken to reach 80-90% confluency) 36

Figure 6 – Residual survival fractions as represented through fitted curves following the induced-repair model. Green curves represent cells exposed to Cs-137 and their progeny while black curves represent cells exposed to Ra-226 and their progeny. The darkest/solid curve represents the initial survival of progenitors directly receiving radiation, the medium/dashed curve represents the first observation of progeny (not directly irradiated), and the lightest/dotted curve represents the second observation of progeny (not directly irradiated). Note significant overlap in residual survival of cells exposed to Cs-137 and their progeny due to minimal observed cell killing. There were roughly 40 days between observations (time taken to reach 80-90% confluency) 38

Figure 7 – Calculated relative effect of alpha particle exposure on residual survival of CHSE-214 cells, as a function of effective gamma dose to progenitor cells. The darkest/solid curve represents the initial survival of progenitors directly receiving radiation, the medium/dashed curve represents the first observation of progeny (not directly irradiated), and the lightest/dotted curve represents the second observation of progeny (not directly irradiated)..... 40

Figure 8 – Proposed experimental setup to observe bystander signals from the progeny of irradiated cells. The lighter portion of the diagram is identical to the lethal mutation experimental setup. Yellow lines indicate culture medium transfer from donor flasks immediately following subculturing. The above would be replicated for each dose observed 56

Figure 9 – Responses to the questions "How much do you trust the regulation of …?", as a function of "How safe would you consider nuclear energy?". Examples were

given for each level: Southern Ontario – Ontario Power Generation, Canada – Canadian Nuclear Safety Commission, Global – International Atomic Energy Agency 60
Figure 10 – Responses to the question "How compliant would your neighborhood be to evacuation instructions in the event of a nuclear accident at the Pickering Nuclear Generating Station?" as a function of "How strong is the feeling of togetherness or closeness in your neighborhood?" 61
Figure 11 – Responses to the questions "If there were a major concern regarding the Pickering Nuclear Generating Station, how likely would it be for community members to get together to jointly petition or address the issue?" as a function of "Do you feel that you have the power to make important decisions that can change the course of your life?" 62

LIST OF TABLES

Table 1 – The lethal mutation phenotype as seen through reduced cloning efficiencies following γ-irradiation. There were roughly 7 days between observations (time taken to reach 80-90% confluency) 20

Table 2 – Statistical analysis of the difference in mean residual survival fractions of progeny at different intervals following γ-irradiation 21

Table 3 – Isolating the relative effect of alpha exposure to the residual survival of HaCaT cells. At each dose, "Expected Residual Survival due to γ" was calculated using the gamma component of the dose, and the function representing residual survival of cells exposed to Cs-137. This was then compared to the residual survival observed when cells were exposed to Ra-226. The difference (Δ) is the isolated effect of alpha exposure. Note negative difference values indicate higher survival of cells in the presence of alpha particles, versus gamma exposure 35

Table 4 – Isolating the relative effect of alpha exposure to the residual survival of CHSE-214 cells. At each dose, "Expected Residual Survival due to γ" was calculated using the gamma component of the dose, and the function representing residual survival of cells exposed to Cs-137. This was then compared to the residual survival observed when cells were exposed to Ra-226. The difference (Δ) is the isolated effect of alpha exposure 39

CHAPTER 1

INTRODUCTION

1.1 MOTIVATION

When responding to nuclear incidents and accidental releases of radiological material most protocols still rely on probabilistic risk models portraying direct effects of radiation. Human carcinogenesis is often a focus of these models and key assumptions of radiobiological effects still rely on interpolations from cancer incidence and mortality rates of the Japanese atomic bomb survivor Life Span Study (LSS) cohort (Hall & Giaccia, 2006). However, doses observed during nuclear incidents/accidents are orders of magnitude lower than those observed following atomic bombings. At lower doses the observed behaviors of cells are dominated by effects that are not in direct response to insult by radiation but are instead the result of complex mechanisms.

The purpose of this thesis is to investigate low dose phenomena including lethal mutation, hyper radiosensitivity and increased radioresistance. It will outline differences in cell survival compared to what is expected from the Linear No-Threshold (LNT) hypothesis in doses where repair processes dictate survival. Further study will investigate variance in

behavior when exposed to different radiation qualities at low doses as well as differences due to cell line and species type. Through outlining indirect consequences of radiation exposure in doses relevant to nuclear incidents/accidents, better understanding can hopefully result in more effective decision-making tools.

1.2 BACKGROUND

When communicating unplanned exposures of radiation to individuals and the environment, regulatory bodies often use the International Nuclear and Radiological Event Scale (INES) to describe in consistent terms the safety significance of an event. The scale classifies events into seven levels. Those that do not cause "actual consequences" but affect measures to prevent and cope such as radiological barriers and controls are termed "incidents" (Levels 1-3: 'anomaly', 'incident', 'serious incident'). In contrast those with serious impacts threatening the safety of people, the environment and/or facilities are deemed "accidents" (Levels 4-7: 'accident with local consequences', 'accident with wider consequences', 'serious accident' and 'major accident' (IAEA, 2013).

While doses received from military nuclear applications are often incomparable to doses from nuclear incidents/accidents, risk estimates

computed from the linear modelling of cancer incidence among survivors of atomic bombings have proved useful in describing radiation related risk of carcinogenesis at more relevant lower doses (Pierce & Preston, 2000). As such it has been the primary basis for the LNT hypothesis which suggests any exposure to radiation increases the risk of stochastic effects, particularly the risk of developing cancer, in a linear fashion proportionate to dose (ICRP, 2007). Reports by scientific committees such as the National Research Council Committee on the Biological Effects of Ionizing Radiation (BIER) and the United Nations Scientific Committee on the Effects of Atomic Radiation (UNSCEAR) contain quantitative risk estimates in agreement with the LNT hypothesis. In turn these reports have largely influenced radiation risk and protection guideline recommendations from international regulatory bodies including the International Commission on Radiological Protection (ICRP). As these recommendations often require pragmatic judgment, the straight-line dose response is deemed practical for the purposes of safety as even in cases of discrepancy, risk is often overestimated (Boice, 2017).

In addition to human epidemiological data, the LNT hypothesis also relies on biological assumptions in line with 'target theory' which suggests the requirement of a direct hit by radiation for an effect, or death (Elkind, 1984). Following this, studies have attempted to depict exposure of

radiation as a direct trigger to tumor initiation, tumor promotion or malignant progression, however it has been shown that radiation can affect all phases depending on the dose, receptor and general state of the target cell (Burtt, et al., 2016). Further, responses in unirradiated progeny and neighbors of irradiated cells have been well documented and are collectively known as non-targeted effects (NTE). While at higher doses these effects rarely cause survival outcomes to vary from what is expected, the results of countless in-vitro studies have suggested that most, if not all low-dose survival is dictated through non-targeted cellular and genomic responses (Seymour & Mothersill, 2000). This is perhaps in part due to differences in gene expression, with greater upregulation of genes concerning cell proliferation and apoptosis at higher doses, compared to responses to low dose radiation involving genes regulating development, intercellular signaling, signal transduction and DNA damage responses (Ding, et al., 2005). As such, the use of signaling and altered repair to cause different levels of mutation and carcinogenesis relative to spontaneous levels have been put forward as justification for modifying the currently accepted LNT hypothesis (Scott, et al., 2003).

Observed NTE are often categorized into two main types. Instances where cell signaling pathways cause radiation-like effects in cells that did not receive direct energy deposition from the ionizing track are referred to

as bystander effects. Genomic instability on the other hand refers to instances where damage does not cause direct mortality and cells appear completely normal, however an increased acquisition rate of alteration or mutation in the genome is transmitted vertically and de novo effects are seen in distant progeny. In some instances, lethality is observed generations later, often referred to as lethal mutation.

Expressions of genomic instability have been observed in experiments dating back to the early 1980s. In 1986, Seymour and Mothersill provided the first formal evidence for de novo damage in descendants through observing lower than expected progeny survival, coining the term "lethal mutations" (Seymour, et al., 1986). Weissenborn and Streffer later irradiated mouse embryos with X-rays in vivo and presented observations of chromosomal aberrations in first and second mitosis post irradiation in 1989 (Weissenborn & Streffer, 1989). By 1992, Kadhim et al boldly implicated the observed high frequencies of non-clonal aberrations in descendants to the transmission of chromosomal instability to progeny, in a paper published in *Nature* (Kadhim, et al., 1992). Through the years further studies have described a wide variety of delayed effects in progeny cells including delayed mutation and transformation, even expressed many generations following exposure (Morgan, et al., 1996).

The studies covered in this thesis focus on endpoints such as lethal mutations relating to genomic instability however it would be incorrect to completely dissociate such responses from the processes of bystander effects. Although further research is still required to define the absolute pathways dictating NTE, a growing consensus agrees on the involvement of chronic inflammation and epigenetics (Lorimore, et al., 2003). Consider the case where a cell receiving direct ionizing radiation employs cell-cell communication to promote the generation of reactive oxygen species (ROS) in its unirradiated neighbors. The production of ROS is thought to be a key mechanism behind the expression of mutations in bystander cells (Bishayee, et al., 2001). However, innate immune processes may also respond to the released ROS and inflammatory mediators, to cause downregulation of cell cycle checkpoints and DNA repair pathways (Colotta, et al., 2009). Signaling could additionally result in instability events in unirradiated progeny, expressed through remarkably higher frequencies of genetic changes such as mutations, chromosomal abnormalities or cell death compared to what would be expected from mutation in a single gene (Kadhim, et al., 2013). In contrast to target theory, where genetic changes of a single irradiated cell would predict clonal changes in progeny, it is thought that epigenetic changes such as DNA methylation explain why genomic damage observed in progeny cells

are non-clonal, as they do not involve alterations to the DNA sequence (Aypar, et al., 2010).

1.3 PURPOSE

While the lethal mutation phenotype has been observed in several cell lines, there is interest in its expression in malignant cells. Following the hypothesis that atypical low dose behaviors observed in malignant cell lines are due to defective DNA repair processes, the preservation of the lethal mutation phenotype across generations may also differ from normal human cell lines. Therefore, Chapter 2 follows the observation of genomic instability through the occurrence of lethal mutation in a human glioma cell line with metastatic potential.

In the context of nuclear incidents and accidental release it is also useful to consider that organisms can be exposed to a variety of radiation qualities. It is therefore important to investigate low dose phenomena when exposed to particulate radiation. Linear energy transfer (LET) is often used to differentiate radiation types as it describes the amount of energy deposited to the interacting material, per unit of distance. Photons such as gamma rays are able to traverse great distances unchanged before being absorbed, however monoenergetic ions such as alpha particles cause

frequent direct ionizations within a smaller range. Due in part to the clustered nature of damage caused, the relative biological effectiveness (RBE) of an alpha particle is often described to be significantly higher than that of a gamma ray. This is a result of the concentration of damage given the same amount of absorbed energy (Goodhead, 1994).

While this may be true for high doses, it has been shown that if a single alpha particle traverses a cell, it causes zero to small risk of oncogenic transformation (Miller, et al., 1999). Further, the work of Nagasawa and Little has shown significantly higher frequencies of mutation than would be expected through linear extrapolation from data for high doses, at doses where the mean number of alpha particle traversals per nucleus was significantly less than one (Nagasawa & Little, 1999). Currently accepted recommendations for the radiation weighting factor (w_r) of alpha particles, which apply the concept of RBE to derive equivalent dose, are dose independent (Wrixon, 2008). However, research has shown instances for RBE to be dose dependent when high dose biological effects are substantially different to low dose effects (Higley, et al., 2012).

The third chapter of this thesis studies whether NTE amplify low dose effects such that they are higher than what would be expected from established LNT related RBE values following exposure to low doses of an

environmental alpha emitter: radium-226. This chapter was adapted from an article submitted on September 17th, 2018 to the PLOS ONE journal titled "Relative biological effect of alpha particle radiation on low dose phenomena: lethal mutation, hyper-radiosensitivity and increased radioresistance", co-authored by Dr. Xiaopei Shi, Dr. Soo Hyun Byun, Dr. Colin B. Seymour and Dr. Carmel E. Mothersill.

1.4 CELL CULTURE

The studies described in this thesis follow the lethal mutation phenotype assayed as reduced cloning efficiency in cultures of human and fish cell lines. The first cell line of interest (Chapter 2) is a human glioma cell line (T98G) transformed to exhibit immortality and anchorage-independence (Stein, 1979), signatures of human tumors with metastatic potential (Mori, et al., 2009). Experiments described in Chapter 3 will observe a human keratinocyte cell line (HaCaT). In addition, due to the increasing relevance of protecting non-human biota from radium in hydrogeologic contaminations from mining, etc., this study will also investigate relative alpha exposure effects in the embryonic Chinook salmon cell line (CHSE-214).

In all studies, reduction in cloning efficiency was observed using the clonogenic assay technique developed by Puck and Marcus (Marcus, et al., 1956). Cell stocks were maintained in T75 flasks with 30ml medium. Upon reaching 80-90% confluence, flasks were subcultured. Here cells were gently rinsed with calcium and magnesium-free DPBS in a biosafety level 2 laminar flow cabinet. The cells were then detached from the flasks according to the specific requirements of the cell using a solution containing trypsin. Once the cells were detached, trypsin was neutralized using fresh culture media and the cell solution was centrifuged at 125g for 4 minutes. The pellet was resuspended, and the cells were counted. The cells were then seeded into fresh flasks with fresh culture media at the

Figure 1 – Following staining using diluted Fuchsin-Carbol, colonies with more than 50 cells are distinctly visible allowing for counting without the use of a microscope

required cell density such that at least 100 viable colonies could be expected to form in control flasks.

Reporter T25 flasks were maintained in the incubator for 9 days. It was experimentally determined that following this incubation period, colonies in sham irradiated (control) flasks were visible to the naked eye. Flasks were stained using 1:4 (v/v) dilution of Fuchsin-Carbol (Ricca Chemical Co., Arlington TX) in water, and macroscopically visible colonies (confirmed to have more than 50 cells when observed under a microscope) were scored as survivors (Figure 1).

1.5 EXPERIMENTAL SETUP

To follow the lethal mutation phenotype, experiments had to observe the cloning efficiency of unirradiated progeny cells compared to progenitor cells receiving direct irradiation. This was done using the experimental setup described in Figure 2. In general, two types of flasks were maintained throughout the duration of the experiment: donor flasks and reporter flasks. Reporter flasks contained colonies that were counted to give clonal efficiency, and thereby survival. These flasks were maintained in triplicates to improve reliability in the recorded observations. Donor flasks worked

similar to cell stocks containing the observed cells and their progeny through the experiment.

For each dose at the initial irradiation, one donor flask and three reporter flasks were prepared to contain 500 cells each. Following irradiation, the three reporter flasks were incubated and stained as described in the previous section. Cloning efficiencies observed in these reporter flasks represented the initial plating efficiencies from direct irradiation. The donor flask was left to incubate until 80-90% confluent, after which it was subcultured as previously described. Again, one donor and three reporter flasks were prepared to contain 500 cells each however there was no further irradiation to be done from this point onwards. The process was repeated, and cloning efficiencies observed in these reporter flasks represented survival fractions of the progeny (P2 and P3). It is assumed the cells in these flasks have not received direct exposure to radiation.

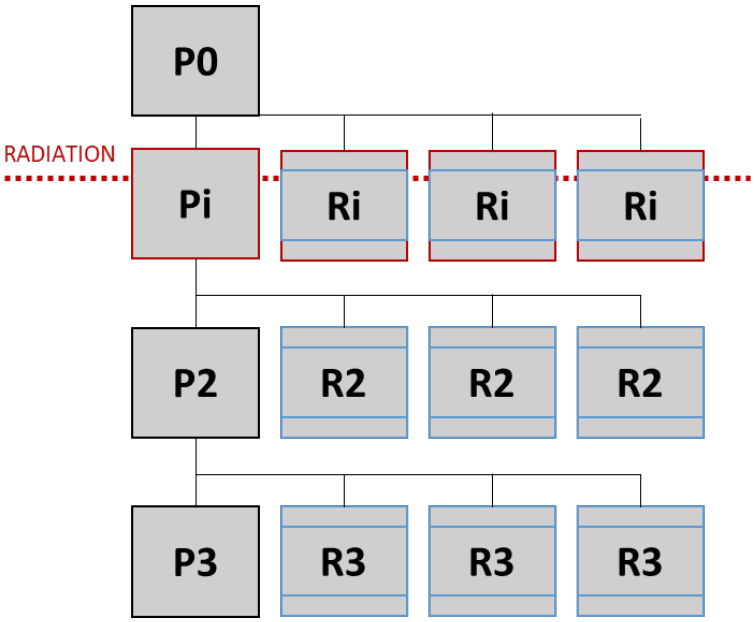

Figure 2 – Diagram describing the general experimental setup for lethal mutation experiments. Flasks marked with 'R' (blue) are reporter flasks while flasks marked with 'P' (black) are donor flasks. Only cells in the initial passage receive direct irradiation. The above is replicated for each dose observed

CHAPTER 2

LETHAL MUTATIONS IN A HUMAN GLIOMA CELL LINE WITH METASTATIC POTENTIAL

The study described in this chapter investigated the expression of the lethal mutation phenotype with respect to dose and time in a human glioma cell line (T98G) transformed to exhibit immortality and anchorage-independence. T98G has previously shown interesting complexities to otherwise well-characterized NTE, such as a reduction in bystander effect between 0.5 and 2Gy. Its behavior is in line with other malignant cell lines that are equally radioresistant to 2Gy doses such as HGL21 and RT112 (Mothersill, et al., 2002).

At low doses (<1 Gy) the T98G cell line exhibits a region of increased sensitivity to acute doses of radiation, termed hyper-radiosensitivity (HRS), followed by a region of increased radioresistance (>~0.7 Gy), termed increased radioresistance (IRR) (Short, et al., 1999). In this region, the effect of irradiation is substantially underestimated by the linear-quadratic model (LQ) and is better described using the induced repair (IR) model (Joiner, et al., 2001). Study has suggested the mechanism behind this

phenomenon to be the ability for these cells to, at low doses, evade an early G2 checkpoint thereby increasing the likelihood of apoptosis (HRS). As increasing doses cause increasing levels of DNA damage, it is able to trigger the checkpoint allowing for effective repair (IRR) (Fernet, et al., 2010). Many tumor cells lack a G1/S cycle checkpoint and are therefore more dependent on G2/M checkpoints to control DNA repair. This suggested mechanism linking enhanced sensitivity to the evasion of ATM-dependent repair processes have been central in investigating ultra-fractionation of dose, to doses in the HRS region, to potentially have therapeutic advantages against radioresistant tumors (Schoenherr, et al., 2013).

The T98G cells were exposed to γ irradiation in doses ranging from 0.5Gy-10Gy and cultured for up to 18 population doublings. The lethal mutation phenotype was followed in the progeny of the initially irradiated cells and measurements were made of their cloning efficiency at intervals to reflect lethal damage in the progeny. The progeny of cells initially irradiated with 0.5Gy remained unaffected but descendants of cells exposed to higher doses expressed a constant rate of reduced clonal efficiency with respect to dose and time. The dose response relationship for lethal mutations observed in T98G was similar to previous experiments in HPV-G cells however the rate of lethal mutation with respect to time was

markedly lower. This supports previous experiments showing atypical non-targeted effects in malignant cells.

2.1 CELL CULTURE

The T98G cell line used in this study were obtained as a gift from Prof. Brian Marples, (Department of Radiation Oncology, William Beaumont Hospital, Royal Oak, MI). The cell line was routinely maintained with Dulbecco's modified Eagle medium F12 (DMEM/F12) + L-glutamine + HEPES (Gibco®, Oakville, Canada), supplemented with 10% fetal bovine serum (FBS; Gibco).

The clonogenic assay technique developed by Puck and Marcus (Marcus, et al., 1956) was used as described in Chapter 1.3. T98G cells were detached using a 0.25% (v/v) trypsin-0.53 mM EDTA solution (Gibco). Cells were counted in this study using an automatic cell counter model Z2 (model Z™ 2; Beckman Coulter Inc., Fullerton, CA).

2.2 ACUTE IRRADIATION USING A CS-137 SOURCE

One set of control T25 flasks to receive 0Gy and four sets of T25 flasks to receive 0.5Gy, 1Gy, 5Gy and 10Gy respectively were seeded and

left to incubate for 6 hours. As described in Chapter 1.4, a set for each dose refers to one donor flask and three reporter flasks. The flasks were then exposed to their respective γ-ray dose using a cesium-137 source (Taylor source, McMaster University, Hamilton, Canada). Flasks were placed at 26 cm from the radiation source, irradiated at a dose rate of 0.273 Gy/min and the room temperature was around 26°C.

All flasks were placed back in the incubator immediately after irradiation. Reporter flasks were incubated and stained as described in Chapter 1.3. The fraction of colonies formed from the 500 cells plated was deemed the initial plating efficiency from direct irradiation. The donor flasks were incubated for 7 days (6 population doublings) to reach 80-90% confluence after which an additional set of flasks were seeded with 500 cells. The reporter flasks were incubated for 9 days and then stained as done prior. Donor flasks were incubated for 7 days before repeating the process for another passage. Each experiment followed 18 population doublings following the initial radiation.

2.3 QUANTITATIVE METHODS

Cloning efficiency of the observed cultures were quantified through survival fractions, where the number of colonies observed in reporter flasks

was divided by the number of cells seeded, corrected for plating efficiency. In addition, the residual survival was calculated at each observed interval, for each dose through following the recorded cell numbers at the start and end of each interval. Here, the product of the cells observed at the end of the current passage, with the total cell number at the end of the preceding passage, is divided by the initial number of cells seeded per passage corrected for plating efficiency.

Following the observation of the lethal mutation phenotype at different time intervals following initial insult from radiation, statistical analysis was done to further describe the significance of damage seen in the clonogenic survival of plated progeny. Using the R Project for Statistical Computing (R Development Core Team, 2008), the mean residual survival at each observed interval was compared to the initial mean survival fraction through an analysis of variance (ANOVA) and a further post-hoc Tukey multiple comparisons of means test at a 95% family-wise confidence level.

2.4 RESULTS

Mean survival fractions and residual survivals are described in Table 1. At 0.5Gy, the colony-forming efficiency of progeny was not greatly

affected. However, as doses increased to 1.0Gy and 5.0Gy, a particular decrease in residual survival is observed especially at the third observation of progeny (*P4, 18 population doublings*). The difference in means between the residual survival of progeny and the initial survival fraction is shown as a percentage of the mean with its respective statistical significance in Table 2. Following an initial dose of 0.5Gy, the cloning efficiency decreased by only 11% ($p=0.99$) by the first observation of progeny (*P2, 6 population* doublings), 6% ($p=0.99$) by the second observation (*P3, 12 population* doublings) and 16% ($p=0.98$) by the third observation (*P4, 18 population* doublings), further confirming little to no difference in the observed progeny. A constant trend of reduction in clonal efficiency is seen from 1Gy onwards. At 10Gy, a statistically significant difference is seen even at the first observation (*P2*) of 75% ($p=0.0015$). This is maintained in subsequent observations: *P3* – 88% ($p=0.0005$), *P4* – 100% ($p=0.0004$).

Table 1 – The lethal mutation phenotype as seen through reduced cloning efficiencies following γ-irradiation. There were roughly 7 days between observations (time taken to reach 80-90% confluency)

Dose to progenitors (Gy)		Mean Survival Fraction	Mean Residual Survival Fraction
0	*initial*	1.00	1.00
	P2	1.00	1.00
	P3	1.00	1.00
	P4	1.00	1.00
0.5	*initial*	0.81 ± 0.01	0.81 ± 0.01
	P2	0.90 ± 0.06	0.72 ± 0.20
	P3	1.05 ± 0.04	0.76 ± 0.30
	P4	0.87 ± 0.06	0.68 ± 0.40
1.0	*initial*	0.76 ± 0.01	0.76 ± 0.01
	P2	0.80 ± 0.05	0.60 ± 0.20
	P3	0.84 ± 0.03	0.50 ± 0.20
	P4	0.86 ± 0.06	0.46 ± 0.30
5.0	*initial*	0.55 ± 0.03	0.55 ± 0.03
	P2	0.79 ± 0.06	0.43 ± 0.10
	P3	0.69 ± 0.04	0.34 ± 0.20
	P4	0.62 ± 0.07	0.24 ± 0.20
10.0	*initial*	0.08 ± 0.01	0.08 ± 0.01
	P2	0.25 ± 0.04	0.02 ± 0.01
	P3	0.34 ± 0.02	0.01 ± 0.002
	P4	0.70 ± 0.08	0.004 ± 0.003

± standard deviation

Table 2 – Statistical analysis of the difference in mean residual survival fractions of progeny at different intervals following γ-irradiation

Dose to progenitors (Gy)		Difference in mean Residual SF (%)	p adj
0	*P2 – initial*	0	-
	P3 – initial	0	-
	P4 – initial	0	-
0.5	*P2 – initial*	-11%	0.99
	P3 – initial	-6%	0.99
	P4 – initial	-16%	0.98
1.0	*P2 – initial*	-21%	0.93
	P3 – initial	-34%	0.78
	P4 – initial	-39%	0.69
5.0	*P2 – initial*	-24%	0.94
	P3 – initial	-38%	0.79
	P4 – initial	-56%	0.56
10.0	*P2 – initial*	-75%	0.0015
	P3 – initial	-88%	0.0005
	P4 – initial	-100%	0.0004

2.5 DISCUSSION

The results of this study can be compared to cultures of an immortalized human keratinocyte cell line known to express high levels of lethal mutations (HPV-G), where reduced colony-forming efficiency was also observed in progeny of cells surviving 1 – 3Gy γ irradiation in a dose-dependent manner, but not 0.5Gy (Mothersill, et al., 2000). The reduction occurred at a greater rate however of 15-20% clonogenic cell loss per

population doubling for HPV-G cells, compared to 2-3% loss per population doubling for T98G cells even at the highest tested dose of 10Gy.

The T98G human glioma cell line used in this study is unique in that it is able to become arrested in G1 phase under stationary phase conditions like normal cells, and yet exhibit transformed characteristics of anchorage independence and immortality (Stein, 1979). Previous studies have also shown the T98G cell line to show low-dose hyper-radiosensitivity (HRS) and increased radioresistance (IRR) [(Short, et al., 1999), (Joiner, et al., 2001)]. It is therefore expected for T98G cells to show lower than expected survival at doses below 1 Gy (hyper-radiosensitivity) compared to the linear-quadratic model, followed by lower than expected cell death (radioresistance) at higher doses. Like many other malignant, rapidly proliferating tumor lines (such as HGL21, RT112 and PC3) this hyper-radiosensitivity/radioresistance is combined with reduced bystander effect noting the correlation of a cell's ability to communicate damage signals, to non-targeted effects (Mothersill, et al., 2002). In comparison, the HPV-G cells while immortalized are not able to exhibit anchorage-independent growth (Chen, et al., 1993). Further, this human keratinocyte cell line is able to exhibit greater bystander effect and does not show hyper-radioresistance (Ryan, et al., 2009).

CHAPTER 3

RELATIVE BIOLOGICAL EFFECT OF ALPHA PARTICLE RADIATION ON LOW DOSE PHENOMENA

At high doses, the current recommended radiation weighting factors advise a significantly higher effectiveness of alpha particles relative to gamma radiation. However, at lower doses, the ratio of effectiveness between radiations of varying linear energy transfer values is complicated due to the relative importance of low dose phenomena such as genomic instability, bystander effects, low dose hyper-radiosensitivity and increased radioresistance (HRS/IRR).

Radium is a common source of alpha radiation exposure to humans, but the dosimetry is complicated by the decay chain which involves gamma exposure due to radon daughters. The study described in this chapter aimed to isolate the relative biological effect of alpha particles after low doses of radium to cells and their progeny. This was done by subtracting the survival values of a human keratinocyte cell line (HaCaT) and an embryonic Chinook salmon cell line (CHSE-214) exposed to gamma irradiation, from survival of the same cell lines exposed to mixed alpha and

gamma irradiation through chronic exposure to Ra-226 and its decay products.

The human cell line showed increased radioresistance when exposed to low doses of alpha particles. In contrast the fish cell line, which demonstrated radioresistance to low dose gamma energy, demonstrated increased lethality when exposed to low doses of alpha particles. The results confirm the need to consider the dose-response relationship when developing radiation weighting factors for low dose exposures, as well as the need to be aware of possible cell line and species differences.

3.1 CELL CULTURE

The HaCaT cell line is an immortalized human keratinocyte cell line originally derived and characterized by Boukamp et al (Boukamp, et al., 1988). The cell line used in this study was obtained as a gift from Dr. Orla Howe (Dublin, Ireland). The cell line was routinely maintained with RPMI-1640 medium supplemented with 10% fetal bovine serum (Invitrogen, Burlington, Canada), 5 ml of 200 mM L-Glutamine (Gibco, Burlington, Canada), 0.5 g/ml hydrocortisone (Sigma-Aldrich, Oakville, Canada), 25 mM Hepes buffer (Gibco), penicillin and streptomycin (Gibco). These cells were grown at 37°C in an incubator with 5% CO^2.

The CHSE-214 is an embryonic cell line derived from Chinook salmon obtained as a gift from Dr. Neils Bols (Waterloo, Canada). CHSE-214 cells were cultured by Dr. Xiaopei Shi in Leibovitz's L-15 medium supplemented with 12% fetal bovine serum (Invitrogen), 5 ml of 200 mM L-Glutamine (Gibco), 25 mM Hepes buffer (Gibco), penicillin and streptomycin (Gibco). These cells were grown at 19°C in an incubator without CO^2.

Similar to the experiments described in Chapter 2, reduction in cloning efficiency was observed using the clonogenic assay technique developed by Puck and Marcus (Marcus, et al., 1956) as described in Chapter 1.3. The HaCaT cells were detached using a 0.25% (v/v) trypsin-1 mM EDTA solution (Gibco) at 37°C for 8 minutes, while CHSE-214 cells were detached using a 0.125% (v/v) trypsin-1 mM EDTA solution (Gibco) at 19°C for 8 minutes. Cells were counted in this study using an automated cell counter (Bio-Rad TC20).

3.2 CHRONIC IRRADIATION USING Ra-226 IN MEDIUM

Dr. Xiaopei Shi conducted the cell preparation, Ra-226 irradiation, clonogenic assay and data collection described in the following section. The

results of these experiments have been previously submitted as part of a doctoral thesis (Shi, 2016).

Stock solutions of medium containing the radioisotope Ra-226 were prepared using neutralized radium nitrate (Eckert and Ziegler, Valencia, USA). 100 ml L-15 or RPMI medium was mixed with 1000 Bq of Ra-226 solution. The concentration of Ra-226 in this stock medium was 10,000 mBq/ml. After filtering into storage tubes, serial dilutions were made to give the required final concentrations.

500 cells were initially seeded into sets of T25 flasks containing 5 ml of medium with Ra-226 or control medium. Sets were prepared as described in Chapter 1.4 (one donor flask and three reporter flasks) for each respective concentration: 0, 0.1, 1, 10, 100, 200 or 500 mBq/ml Ra-226. Flasks were maintained in the incubator for 9 days after which the radioactive medium was removed, and the cells were gently rinsed with calcium and magnesium-free DPBS. Ra-226 residues in the flasks were assumed to be insignificant. Flasks then received 5 ml of fresh culture medium without Ra-226 and returned to the incubator. Reporter flasks were incubated and stained as previously described. Cloning efficiencies observed in these reporter flasks represented the initial plating efficiencies from direct chronic irradiation. The remaining donor flask of each concentration was left to incubate until 80-90% confluency, after which it

was subcultured as described in Chapter 1.3. From here on however no further irradiation was to be done and all flasks received fresh culture medium containing 0 mBq/ml Ra-226. The process was repeated as before, and cloning efficiencies observed in these reporter flasks represented survival fractions of the progeny. (P2).

3.3 ACUTE IRRADIATION USING A CS-137 SOURCE

As with the Ra-226 experiments, Sets of T25 flasks were seeded with 500 cells for each respective dose: 0, 0.05, 0.1, 0.25, 0.5, 0.75 or 1 Gy. The flasks were incubated for 6 hours to allow for cells to adhere to the flask, after which they were exposed to their respective γ-ray dose using a cesium-137 source (Taylor source, McMaster University, Hamilton, Canada). Flasks were placed at 26 cm from the radiation source, irradiated at a dose rate of 0.273 Gy/min and the room temperature was around 26°C.

All flasks were placed back in the incubator immediately after irradiation. Similar to the Ra-226 experiments, reporter flasks were incubated and stained as described above (initial). Donor flasks were incubated until cells were 80-90% confluent, after which they were

subcultured as described above with fresh culture medium. This process was also repeated twice as above (P2 and P3).

3.4 DETERMINING γ DOSE FROM RA-226

All possible γ emission events during the decay of Ra-226 to daughters Pb-214 and Bi-214 were tabulated according to their energy (keV) and probability (%) (Eckert & Ziegler, 2010). Total γ energy emitted per decay was then found through the summation of each γ energy multiplied by its emission probability. A system was then set up to describe the source geometry: a plane of uniformly spread particles with a y-dimension twice as big as the x-dimension (similar to T-25 flask dimensions), with each particle emitting the γ energy calculated previously. The radionuclide was assumed to be evenly distributed in the medium. As such, the number of particles (N) emitted from the source was calculated through the concentration of Ra-226 in each respective medium (dividing the activity by the decay constant). Radionuclides in the corners of the flask would only contribute dose to 90°, while those immediately adjacent

to the flask walls would only contribute 180° of dose. Figure 3 shows one iteration describing the spatial distribution of γ emissions in a flask.

Dose rate contributed by each particle was calculated using the following equation:

$$\dot{D} = \frac{AE}{4\pi r^2}\frac{\mu_{en}}{\rho}$$

Where A represents the respective activity (Bq), E represents the respective γ energy emitted per decay (MeV) and μ_{en}/ρ represents the mass energy-absorption coefficient (assumed to be 0.05 to represent cells). The final dose was determined in Gy through multiplying the average dose rate for all particles in the flask (determined with consideration to the previously

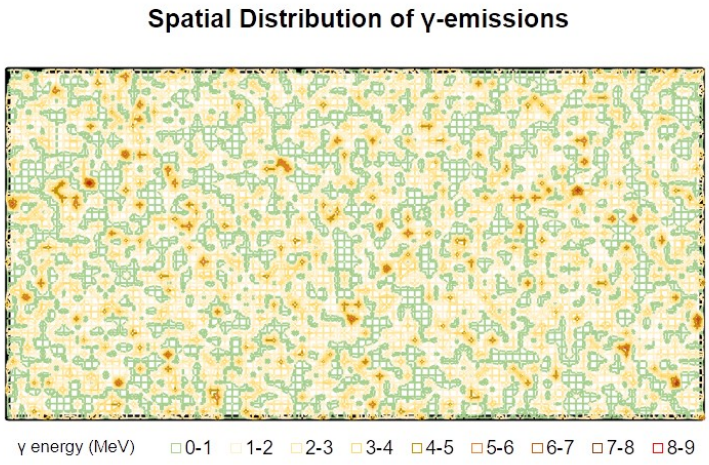

Figure 3 – One iteration of the Monte Carlo simulation determining the spatial distribution of Ra-226 particles emitting gamma energy per emission (500 mBq/ml shown). The gamma energy is shown in MeV according to the legend

defined geometry parameters through Monte Carlo simulation) by the time exposed to Ra-226 (9 days or 7.8×10^5 seconds).

3.5 CURVE MODELLING

Survival fractions/plating efficiencies of cells are determined as cloning efficiency observed through staining: the fraction of colonies formed from the 500 cells plated. Residual survival fractions were calculated at each observed interval and for each dose through following the recorded cell numbers at the start and end of each interval, in accordance to previous delayed lethal effect assays by Mothersill et al. [(Lyng, et al., 1996), (Mothersill, et al., 2000)]. Here, the product of the cells observed at the end of the current passage, with the total cell number at the end of the preceding passage, was divided by the initial number of cells seeded per passage corrected for plating efficiency. Finally, curves were fitted to the calculated residual survival values at each observed interval using the induced-repair equation taken from the model described by Lambin et al. (Lambin, et al., 1993):

$$S = \exp\left(-\alpha_r\left(1 + \left(\frac{\alpha_s}{\alpha_r} - 1\right)e^{-\frac{D}{D_c}}\right)D - \beta D^2\right)$$

Here a_r describes the traditional linear-quadratic dose-response model while a_s describes a region of the curve showing resistance from the linear component. Curves were fit using the R Project for Statistical Computing (R Development Core Team, 2008) through the nlsLM function of MINPACK, which uses a modified Levenberg-Marquardt algorithm to perform non-linear regression. The residual sum of squares (RSS) was used to further observe the fit of the curve to empirical values, as well as verify the use of the induced-repair equation compared to the traditional linear-quadratic model.

To isolate the effect of α-particles on the survival and genomic instability of cells, this study subtracted effects observed after γ irradiation (through acute exposure to Cs-137) from mixed α and γ irradiation (through chronic exposure to Ra-226). Once the empirical data of the study is represented through curves, this is simply done through subtracting the function of one curve from the other.

3.6 RESULTS

HUMAN KERATINOCYTE CELL LINE (HaCaT)

Fitted curves representing the residual survival fractions for HaCaT cells show markedly different responses in directly exposed cells and their

progeny with acute exposure to Cs-137 compared to those with chronic exposure to Ra-226 (Figure 4). Progenitor HaCat cells (initial) exposed to Cs-137 show a region of hyper-radiosensitivity (HRS) at very low doses with lower survival than would be expected by the traditional linear-quadratic model, followed by a region of increased radioresistance (IRR). The progeny of these cells continue to demonstrate such HRS/IRR behavior with further decrease in cloning efficiency thereby observing lethal mutations in those generations. In particular significant decreases in cloning efficiencies are observed in the first observation of progeny of cells (P2, 8 population doublings) irradiated at 0.05 Gy by 19% ($p=0.007$), 0.1 Gy by 23% ($p=0.00007$), 0.25 Gy by 14% ($p=0.02$), 0.5 Gy by 15% ($p=0.01$) and 0.75 Gy by 17% ($p=0.0004$). Further significant decreases are observed in the second observation of progeny (P3, 16 population doublings) at 0.05 Gy by 17% ($p=0.01$) and at 0.1 Gy by 14% ($p=0.001$). The residual sum of squares (RSS) values for the initial, P2 and P3 curves are 0.0003, 0.004 and 0.002 respectively, demonstrating noticeably better fit with the induced-repair equation compared to the traditional linear-quadratic model (RSS values of 0.2, 0.09 and 0.2 respectively).

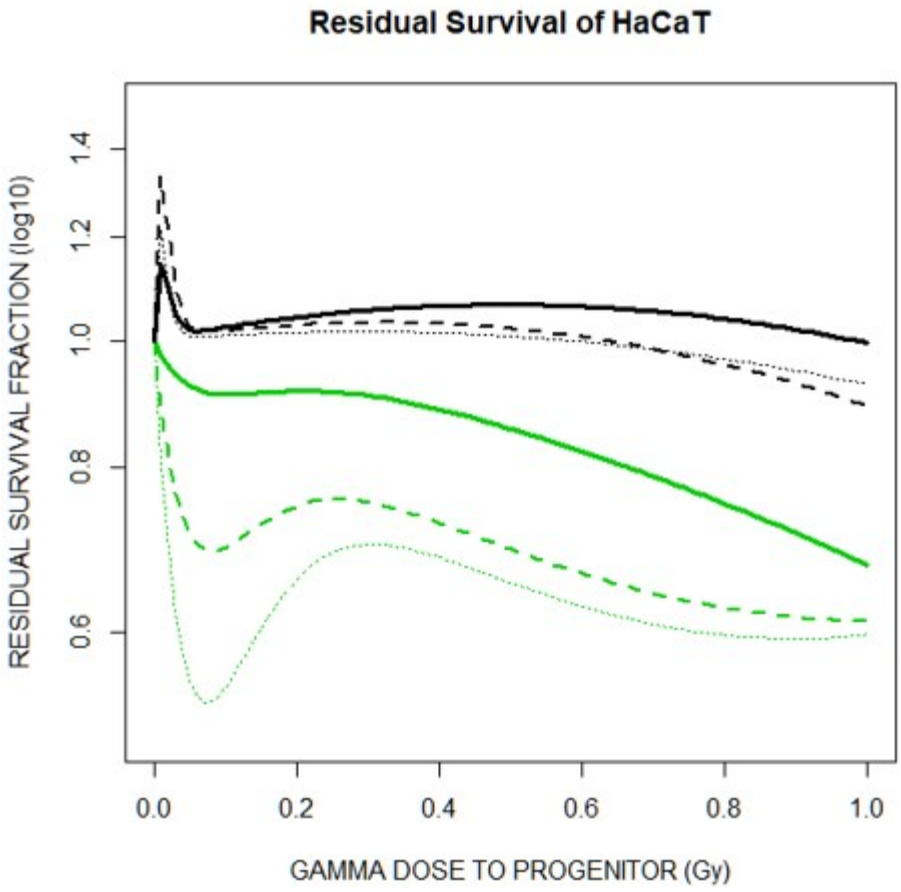

Figure 4 – Residual survival fractions as represented through fitted curves following the induced-repair model. Green curves represent cells exposed to Cs-137 and their progeny while black curves represent cells exposed to Ra-226 and their progeny. The darkest/solid curves represent the initial survival of the progenitors directly receiving radiation, medium/dashed curves represent the first observation of progeny (not directly irradiated), and the lightest/dotted curves represent the second observation of progeny (not directly irradiated). There were roughly 7 days between observations (time taken to reach 80-90% confluency)

In comparison, progenitor cells exposed to Ra-226 show significantly greater survival with many observations of higher cloning efficiency compared to sham irradiated control flasks (denoted as survival values greater than 100%). As such no HRS region is observed, with little to no change in survival compared to control in cells exposed to concentrations greater than 0.1 mBq/ml of Ra-226. At P2, survival of progeny in concentrations up to 10 mBq/ml of Ra-226 observe significantly higher survival compared to control, while observations at P3 show similar survival values to what was observed in the progenitors. Despite lacking an HRS/IRR region, the induced-repair equation still shows greater fit with RSS values of 0.006, 0.03 and 0.005 respectively for the initial, P2 and P3 curves (compared to 0.02, 0.08 and 0.03 respectively for the traditional linear-quadratic model), as it better matches the observed hyper increased radioresistance (HIRR) observed at very low doses.

Through subtracting the functions of fitted curves for cells exposed to Cs-137 from those exposed to Ra-226 at each interval, the relative effect of alpha exposure to the residual survival of HaCaT cells was isolated (see Table 3). Figure 5 describes the functions of the isolated effect of alpha exposure to residual survival graphically at each observation.

Table 3 – Isolating the relative effect of alpha exposure to the residual survival of HaCaT cells. At each dose, "Expected Residual Survival due to γ" was calculated using the gamma component of the dose, and the function representing residual survival of cells exposed to Cs-137. This was then compared to the residual survival observed when cells were exposed to Ra-226. The difference (Δ) is the isolated effect of alpha exposure. Note negative difference values indicate higher survival of cells in the presence of alpha particles, versus gamma exposure

Dose (mBq/ml Ra-226)		Expected Residual Survival due to γ	Observed Ra-226 Residual Survival (γ+α)	Δ
0	*Initial*	1.00	1.00	0.00
	P2	1.00	1.00	0.00
	P3	1.00	1.00	0.00
0.1	*Initial*	1.00	1.09	-0.09
	P2	0.10	1.18	-0.18
	P3	0.99	1.09	-0.10
1	*Initial*	0.99	1.07	-0.08
	P2	0.97	1.16	-0.19
	P3	0.94	1.15	-0.21
10	*Initial*	0.95	1.07	-0.12
	P2	0.79	1.15	-0.36
	P3	0.65	1.06	-0.41
100	*Initial*	0.91	1.04	-0.13
	P2	0.76	1.03	-0.27
	P3	0.69	1.01	-0.32
200	*Initial*	0.86	1.07	-0.21
	P2	0.69	1.13	-0.44
	P3	0.65	1.01	-0.36
500	*Initial*	0.58	0.92	-0.34
	P2	0.62	0.79	-0.17
	P3	0.64	0.86	-0.22

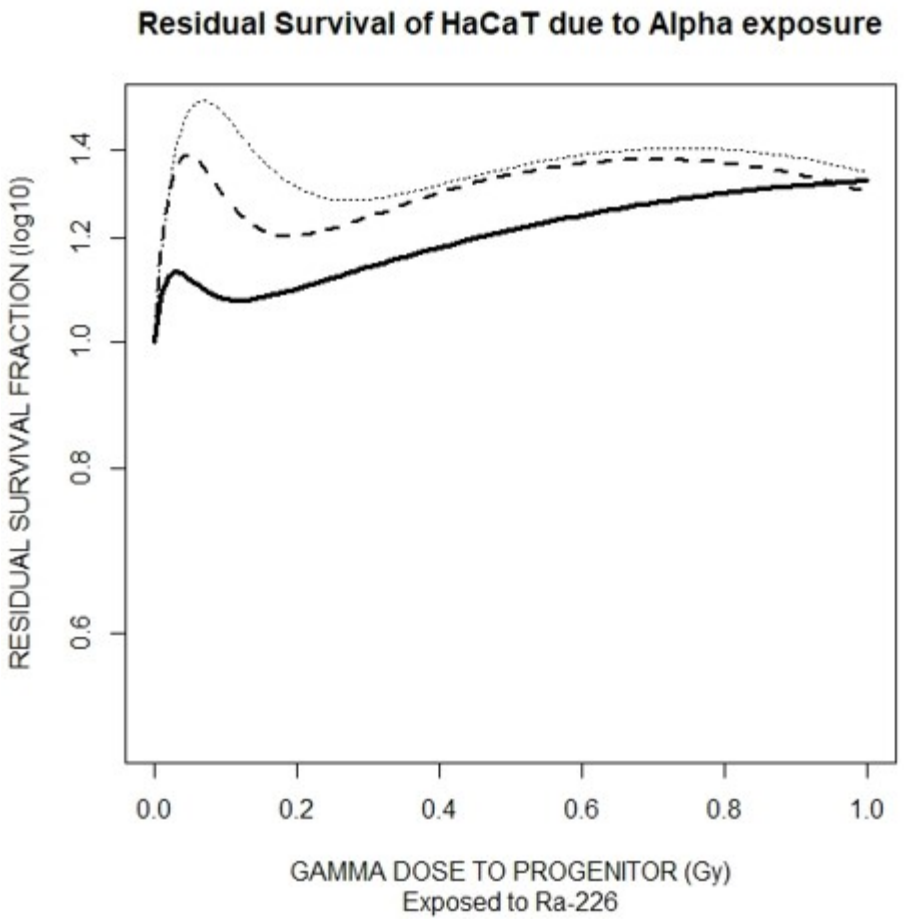

Figure 5 – Calculated relative effect of alpha particle exposure on residual survival of HaCaT cells, as a function of effective gamma dose to progenitor cells. The darkest/solid curve represents the initial survival of progenitors directly receiving radiation, the medium/dashed curve represents the first observation of progeny (not directly irradiated), and the lightest/dotted curve represents the second observation of progeny (not directly irradiated). There were roughly 7 days between observations (time taken to reach 80-90% confluency)

EMBRYONIC CHINOOK SALMON CELL LINE (CHSE-214)

In contrast to the studied human cell line, there was no significant cell death observed in the directly exposed cells of the CHSE-214 fish cell line and their progeny to acute Cs-137 exposure (Figure 6). This shows an existing radioresistance when compared to human cell culture (Ryan, et al., 2008). When CHSE-214 cells were exposed to Ra-226 however, progenitor cells show a marked response with decreasing cell survival following an almost linear trend with respect to dose. Residual survival observed at P2 (8 doubling periods) show increased lethal mutation however residual survival observed in the subsequent progeny at P3 (16 doubling periods) demonstrate a return of radioresistance with survival values similar to initial values.

Using the same methodology as was done for the human cell line, the relative effect of alpha exposure to the residual survival of CHSE-214 cells was isolated (see Table 4). As exposure to gamma irradiation caused little to no effect in residual survival, the isolated relative effect of alpha exposure is significant, especially at the higher end of the low dose range. The dose dependent function for the isolated effect at each observation is shown graphically in Figure 7.

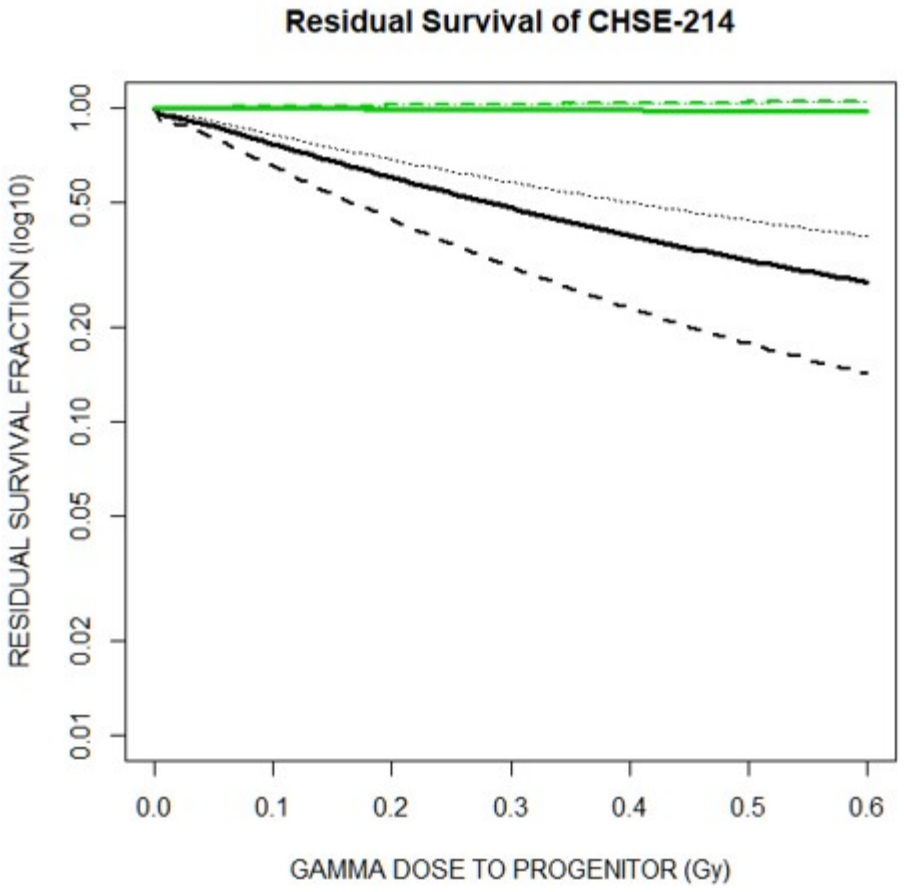

Figure 6 – Residual survival fractions as represented through fitted curves following the induced-repair model. Green curves represent cells exposed to Cs-137 and their progeny while black curves represent cells exposed to Ra-226 and their progeny. The darkest/solid curve represents the initial survival of progenitors directly receiving radiation, the medium/dashed curve represents the first observation of progeny (not directly irradiated), and the lightest/dotted curve represents the second observation of progeny (not directly irradiated). Note significant overlap in residual survival of cells exposed to Cs-137 and their progeny due to minimal observed cell killing. There were roughly 40 days between observations (time taken to reach 80-90% confluency)

Table 4 – Isolating the relative effect of alpha exposure to the residual survival of CHSE-214 cells. At each dose, "Expected Residual Survival due to γ" was calculated using the gamma component of the dose, and the function representing residual survival of cells exposed to Cs-137. This was then compared to the residual survival observed when cells were exposed to Ra-226. The difference (Δ) is the isolated effect of alpha exposure

Dose (mBq/ml Ra-226)		Expected Residual Survival due to γ	Observed Ra-226 Residual Survival (γ+α)	Δ
0	*Initial*	1.00	1.00	0.00
	P2	1.00	1.00	0.00
	P3	1.00	1.00	0.00
0.1	*Initial*	1.00	0.69	0.31
	P2	1.00	0.50	0.50
	P3	1.00	0.66	0.34
1	*Initial*	1.00	0.71	0.29
	P2	1.00	0.56	0.44
	P3	1.00	0.73	0.27
10	*Initial*	1.00	0.75	0.25
	P2	1.01	0.61	0.40
	P3	1.03	0.81	0.22
100	*Initial*	1.02	0.55	0.47
	P2	1.10	0.39	0.71
	P3	1.23	0.64	0.59
200	*Initial*	1.02	0.31	0.71
	P2	1.17	0.15	1.02
	P3	1.39	0.45	0.94

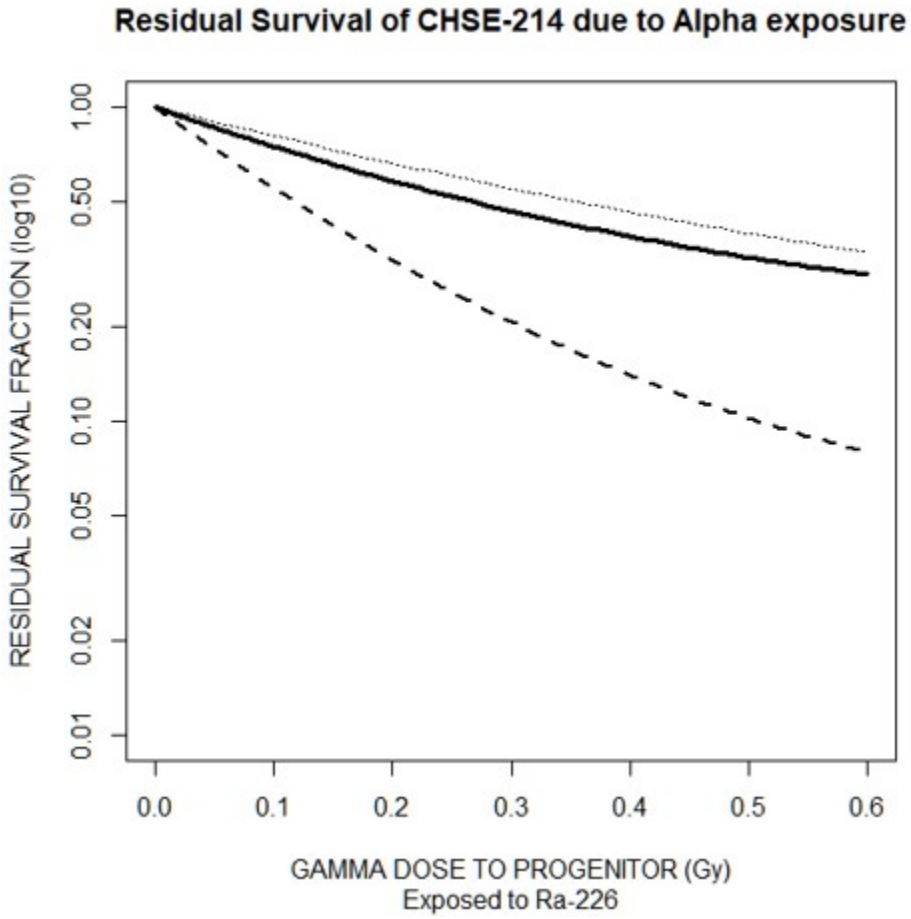

Figure 7 – Calculated relative effect of alpha particle exposure on residual survival of CHSE-214 cells, as a function of effective gamma dose to progenitor cells. The darkest/solid curve represents the initial survival of progenitors directly receiving radiation, the medium/dashed curve represents the first observation of progeny (not directly irradiated), and the lightest/dotted curve represents the second observation of progeny (not directly irradiated)

3.7 DISCUSSION

At sub-lethal doses of gamma irradiation through acute exposure to Cs-137, the HaCaT cell line displayed a region of low-dose hyper-radiosensitivity (HRS) followed by increased radioresistance (IRR). In addition, lethality was observed in subsequent generations (lethal mutation phenotype) with significant decreases in cloning efficiencies observed in unirradiated progeny cells. In contrast, only radioresistance was observed in the progenitor cells exposed to Ra-226 with significantly higher survival and no observable region of HRS. Further, the observed progeny of these cells showed increased survival and lowered lethal mutation. In comparison, the results of experiments using the non-mammalian embryonic fish cell line showed the reverse of what was observed in human cell culture. Survival data following exposure to gamma irradiation confirmed existing radioresistance in the CHSE-214 cell line compared to human cell culture, with no significant lethality. However, survival data for cells exposed to Ra-226 suggested that alpha particles promoted lethality at doses otherwise known to have no significant effect.

Considering the potential for sub-lethal doses from chronic exposure to radium and its daughters found in waste products, to remnants of historic commercial and medical usage of radium (ranging from self-luminous paints to cancer treatment), the unconventional behaviors

observed in both cell lines of this study have potential importance in radiological protection. Further, the presence of radium in waste reaching the ecosystem from mining and nuclear applications is important given the currently growing interest for non-human radiological protection.

The radioprotective quality of sub-lethal doses of alpha radiation that was observed in the HaCaT cell line, where cells displayed significantly lower lethality in the presence of alpha particles greatly contrasts with RBE values found in the literature. Previous in vitro studies of alpha radiation effects at higher doses compared to this study have all consistently demonstrated a significantly higher biological effect of alpha particles relative to photons, with values ranging from <2 for the induction of double strand breaks, to 3.5-10 for cell lethality and transformation in different cell lines, to >25 for other endpoints assessed (Thomas, et al., 2007). Research observing HRS/IRR behaviors suggest the activation of cell cycle checkpoints for increased cell repair, etc. as a possible mechanism for radioresistance (Fernet, et al., 2010). Considering only radioresistance was observed in the presence of alpha radiation, the results suggest an ultra-low dose of alpha particles produces a sufficient level of genomic instability to activate the previously mentioned cell cycle checkpoints, inducing radioresistance. This effect was non-linear with dose with marked reduction as dose increased to the progenitor. The results observed in the

CHSE-214 cell line on the other hand is in line with currently accepted descriptions on the effect of alpha particles at high doses. Here, the concentration of damage events is said to exceed a threshold at which effective repair becomes difficult (Blöcher, 1988). Further lethality is seen in progeny as a de novo appearance of non-clonal lethal mutations, indicative of genomic instability. However, this decreases with subsequent generations suggesting the ability for existing damage repair mechanisms eventually to counteract the heritable susceptibility to lethal damage.

The results of the study support the need to consider dose-dependence when describing the relative biological effect of different radiation qualities. Overestimation of the biological effect of sub-lethal exposure to radium in humans can result in unnecessary psychological stress and limit productivity in industry (Batty, et al., 2017). In addition, the results of the fish cell line experiments confirm the need to be aware of species differences, confirming that protection for humans would not inherently protect ecosystems and non-human biota (Bréchignac, 2002).

It should be noted however that the observed in vitro results cannot simply be translated to in vivo effects without further research. For example, while there is evidence for heritable NTE through in vitro and non-human studies, there has been no evidence for radiation-induced hereditary effects observed in epidemiological studies of human

populations exposed to ionizing radiation (Morgan, 2003). In addition, further research needs to be done to isolate the effect of dose rate on sub-lethal exposure to high-LET radiation, as differences in time for cell repair can affect the level of radioresistance observed.

CHAPTER 4

CONCLUSIONS AND FUTURE DIRECTIONS

4.1 DIRECT EFFECTS

There is sound reason behind using conservative risk estimates for carcinogenesis as a basis for nuclear safety. As a leading cause of mortality in the Western world, cancer has been studied through a variety of lenses. However, this has only confirmed that the etiology of cancer is far more complex than simply a matter of probability. This was demonstrated in the response by the scientific community to a report published in *Science* containing statistical analysis of the division of stem cells among 31 tissue types during an average individual's lifetime. In this report, Tomasetti and Vogelstein reported a high correlation (0.804) between the total number of stem cell divisions and cancer risk. The authors further proposed, through this correlation analysis, that random mutations caused by errors during the division of noncancerous stem cells were implicated for a large majority of human carcinogenesis (Tomasetti & Vogelstein, 2015). At its core, this so called "bad luck" was seen to reduce the impact of hereditary and environmental factors on variation in cancer risk among tissues. The

report itself weighed such extrinsic factors to impact only a third of the variation in cancer risk, attributing the large remaining portion to bad luck.

A great concern with the bad luck proposal was its incompatibility with known risk factors of certain environmental agents on tissue. A study by Little et al. considered radiation-associated and tobacco-associated risks through current models, in describing cancer incidence and mortality from the Japanese atomic bomb survivor LSS cohort, as well as baseline US cancer risk at various sites. Following the assumption that the Extra Risk Score (ERS) found in Tomasetti and Vogelstein's report identified tissue types at higher risk for impact from environmental factors, Little et al. looked to see if ERS could be used as a metric to explain variation in susceptibility of a tissue type to radiation and tobacco. Results however found little correlation between ERS and radiation or smoking associated cancer risk, concluding predictions from the bad luck factor were "in conflict with predictions of a multistate model of carcinogenesis, under the assumption of homogeneity of numbers of driver mutations across most cancer sites" (Little, et al., 2016).

Through their methodology, Little and colleagues also challenged the variable quality of the data used in the original study. Quesenberry and Goldberg refer to similar doubts identifying special cases like lymphocytes

that could be considered potential stem cells when encountering antigens, thereby making estimates of stem cell proliferation unreliable (Quesenberry & Goldberg, 2015). They also considered two confounding factors when attempting to estimate cancer risk by stem cell divisions: the concept of the immortal strand in stem cell biology and the impact of microenvironment on carcinogenesis.

The impact of microenvironment can be best seen in cancers that revert to normal when exposed to different environments. Noble et al. further argued that changes in microenvironment could greatly influence the selective value of mutations, an interaction between the extrinsic environment and intrinsic bad luck factor that was not considered by the model (Noble, et al., 2016). This however suggests that in considering additional factors required in accurately estimating relative contribution to risk, using simple rules would not result in useful risk factors when planning cancer prevention and suppression.

The concept of the immortal strand comes from a hypothesis proposed by Cairns in the 1970s, and further validated experimentally. It suggests that similar to mechanisms in bacteria which keep template strands together, stem cells co-segregate the parental strands into the cell that remains a stem cell so that any errors during replication do not get permanently fixed (Cairns, 2006). Considering the effects of the immortal

strand, one would expect differences in estimates of mutations through division rates. This is further complicated by evidence that mutations in stem cells, while predictable, are not completely stochastic. For example, while 76% of colorectal cancers have a mutated tumor suppressor APC gene, and while 1031 of 2843 codons can be changed to stop codons by a single base substitution, a substantial portion of the nonsense mutations occur at a region representing <3% of the codons (Gold, 2017). Tomasetti and Vogelstein have argued their correlations hold true despite substantial changes in stem-cell divisions (approximately 100-fold changes in either direction) however certain changes may result in different conclusions to how much variation is explained by intrinsic versus extrinsic factors.

Showing that correlation analysis could not distinguish between intrinsic and extrinsic factors, the implication that only a third of variation in risk was due to extrinsic factors in Tomasetti and Vogelstein's original analysis was challenged by Wu et al. who provided a reanalysis of the data using a different mathematical model. In this alternate methodology, Wu et al. estimated a lower bound intrinsic risk line by arguing the cancer with the least risk in the entire group should control for that arisen purely through stem cell divisions. Any higher cancer incidence would therefore reflect extrinsic risk factors. In contrast to the original report, this model suggested intrinsic risk factors only contributed to less than ~10-30% of

lifetime risk, a drastically different conclusion from that made by Tomasetti and Vogelstein (Wu, et al., 2016). It must be noted however that even this alternative analysis is flawed with estimates for extrinsic risks that do not follow what is known from epidemiological and genetic data (Noble, et al., 2016).

It is undeniable that the bad luck proposal had sparked a new way of understanding cancer. New computational models improving from the faults of previous attempts, while also incorporating factors like the concept of the immortal strand have aimed to deliver richer results to better explain external risks associated with agents like radiation or smoking (Little & Hendry, 2017).

In addition, the proposal had found improvement through work in fields beyond computational oncology research. For example, by implicating carcinogenesis as a natural by-product of cellular processes, the bad luck factor had to answer Peto's paradox which notes cancer incidence does not scale with the number of cells in an organism. Peto's paradox is often explained with the lens of evolution, suggesting that natural selection has allowed larger species to have greater levels of cancer protection. With this phenomenon in mind, the data of the original study was reanalyzed to find that variation in cancer risk was best explained when the data was grouped by anatomical site, as each site had very

different risk per stem cell division. This further suggested the evolution of different cancer prevention in different anatomical sites within a body (similar to variation in cancer prevention of different species through natural selection) (Noble, et al., 2015).

The greatest take away from the discussion that followed Tomasetti and Vogelstein's report however was simply that by attempting to represent risk of carcinogenesis through highly simplified probabilistic terms, important contributing factors were often easily lost (Batty, et al., 2017). This is comparable to current nuclear safety protocols that fail to incorporate low dose phenomena. At doses relevant to nuclear incidents and accidents, detriment caused by direct effects (mortality, illness, etc.) are often comparable to those caused by indirect consequences and it is therefore warranted to consider more encompassing responses.

4.2 CELL CULTURE

The results of the studies described in this thesis have shown that at sub-lethal doses, survival greatly depends on repair mechanisms. Experiments observing the delayed effects of γ irradiation on the T98G cell line showed little to no effects in progeny of cells irradiated with 0.5Gy while showing a constant trend of reducing cloning efficiency with respect

to dose and time, after initial exposure to doses greater than 1Gy. It should be noted that the T98G cell line is known to exhibit a region of hyper-radiosensitivity to doses less than 1Gy (Fernandez-Palomo, et al., 2016). This parallels the response of the HaCaT cell line which also demonstrated hyper-radiosensitivity to gamma energy at low doses. The results of the experiments described in Chapter 3 however show that high-LET alpha particle radiation may produce sufficient genomic instability to induce radioresistance in the same dose region. In such instances, the ratio of relative biological damage caused by alpha exposure is significantly lower than an equivalent dose of gamma energy alone, and as such a lower radiation weighting factor could be considered. In contrast, while the CHSE-214 cell line demonstrated increased radioresistance to gamma energy, the concentrated nature of energy deposited caused increased lethality when exposed to alpha particles. These cases would suggest a higher radiation weighting factor, similar to what is currently recommended. Further study is required to isolate the effect of dose-rate at sub-lethal doses. In addition, further consideration is required to translate the observed in vitro results to in vivo effects.

The conclusions of the experiments observed in this thesis are in line with previous research that have shown evidence for a relationship between the effect of radiation quality on the incidence of radiation induced

genomic instability (Smith, et al., 2003). However, determining a concise numerical value such as RBE to communicate the efficacy of inducing instability events by high LET radiation relative to low LET has been difficult due to the range of endpoints and possible underlying systems following exposure. In studies described by Weissenborn and Streffer in the late 1980s following exposures of mouse embryos it was concluded that neutrons were more effective than X-rays at producing chromatid aberrations, observing a value of 7.5 at the third mitosis (Weissenborn & Streffer, 1988). Further study showed similar bias for chromatid-type aberrations versus chromosome-type aberrations in study of human bone marrow cell culture when exposed to alpha particles, while showing virtually no aberrations following exposure to X-rays [(Kadhim, et al., 1992), (Kadhim, et al., 1994)]. This however was not reflected in experiments of the GM10115 human-hamster hybrid cell line which showed little to no sensitivity in response to radiation of varying LET (Limoli, et al., 2000). In addition to the species and cell-type specific differences in response, variation in dose-response was also observed. In the research article describing lethal mutation experiments on the HPV-G cell line by Mothersill et al. (mentioned in the discussion of Chapter 2), increased cell death was observed following 1 and 3 Gy of X-ray irradiation with increased levels of chromosome aberrations and persistent apoptosis. A dose-dependent decrease in plating efficiency was also observed

following the exposure of alpha particles generated by a Pu-238 source. However, while the progeny following x-ray exposure showed eventual decrease in the frequency of persistent apoptosis, the progeny following alpha exposure showed an increased fraction of apoptotic cells that remained at 23% twelve populations later (Mothersill, et al., 2000).

To account for the variance in species and dose response for the endpoints associated with genomic instability at low doses, the relative difference in observed persistent cellular damage following varying radiation qualities can only be quantified once the underlying systemic processes that initiate and perpetuate instability following irradiation is identified. Epigenetics and inflammation are promising candidates however, epigenetic effects are often short lived and do not explain the temporal range of effects observed, sometimes appearing many generations later. Inflammatory and immune responses do not appear in cell culture and therefore there exists an additional means by which the damage event transcends the affected cells. In looking at epigenetic in vivo bystander effects in different organs of the same organism, located equidistant from the exposure field, a difference in loss of DNA methylation was seen between the skin and spleen of mice. Here, discussion of the difference pointed to the involvement of protein complexes, suppressor proteins, protein kinases, protein-related factors and signaling molecules involved

in cell cycle control, proliferation and DNA repair (Ilnytskyy, et al., 2009). While this is a sizeable list, it's possible a complex combination of these molecules modulating the genetic background of the system, underlies the spectrum of aberrations, endpoints and phenotypes observed.

It is also worthwhile to investigate variance in response to differences in cell lines to identify possible candidates. In looking to combat malignancy caused by the anchorage-independent growth of T98G, a study by Haga et al showed significantly lower colony formation in soft agar plates in transformants that expressed and secreted human ST2 protein. The inhibitory effect was dose dependent and reproducible showing strong evidence for the ability of the ST2 protein to suppress anchorage-independent growth. Higher levels of ST2 mRNA in benign tumors compared to lower levels in malignant tumors support the hypothesis that ST2 is used in pathways that combat malignancy (Haga, et al., 2003). ST2 is a member of the interleukin 1 receptor family and is able to activate mitogen-activated protein kinase (MAPK) which are involved in the regulation of proliferation, cell survival and apoptosis, among other roles (Brint, et al., 2004). Studies have shown ST2 to play a central role in innate and adaptive immune responses, for example levels of soluble ST2 have been reported to be increased during sepsis as well as in trauma patients (Brunner, et al., 2004). Recent epidemiology of nuclear workers that were

occupationally exposed to low-dose ionizing radiation also show elevated levels of the activity of soluble receptor ST2 showing a possible link to the secretion of the ST2 protein in response to insult by low-dose radiation exposure (Katsarska, et al., 2016).

Following previous suggestions that relate differences in low-dose radiobiological phenomena in malignant cells like T98G to their reduced ability to communicate damage signals, the results of this study further support reduced production of radiation-induced inflammatory cytokines in malignant cell lines expressing anchorage-independence, as a potential reason for their lower rates of genomic instability and bystander effect. Similar experimentation in malignant cell lines transformed to express genes like the human ST2 protein (as used in the study by Haga et al) could give further insight to the relationship of innate and adaptive immune responses to non-targeted effects.

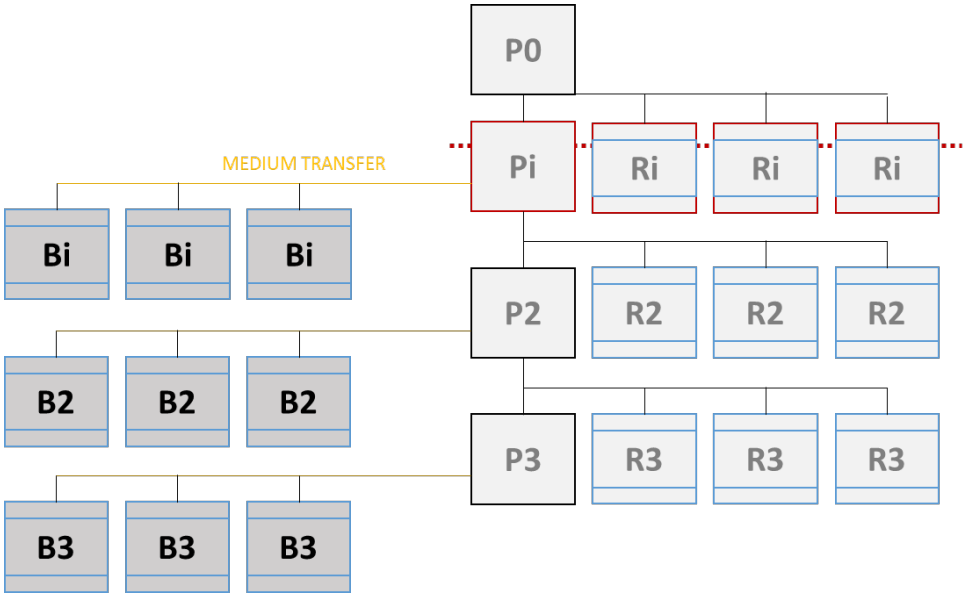

Figure 8 – Proposed experimental setup to observe bystander signals from the progeny of irradiated cells. The lighter portion of the diagram is identical to the lethal mutation experimental setup. Yellow lines indicate culture medium transfer from donor flasks immediately following subculturing. The above would be replicated for each dose observed

Finally, more experimentation is required regarding the interaction of other NTE at low doses. Figure 8 outlines an experimental setup where culture medium is transferred from donor flasks to parallel sets of reporter flasks to observe bystander signals in the progeny of irradiated cells. By gaining a full understanding of mechanisms and behaviors that dictate responses at low doses, more effective decisions can be made to improve safety following nuclear incidents and accidents.

4.3 FURTHER INDIRECT CONSEQUENCES

In addition to NTE from exposure to radiation at the cellular level, nuclear incidents and accidental releases can have indirect consequences in further contexts up to the population level. This is particularly apparent in the wake of nuclear emergencies. Following the 9.0 magnitude earthquake and subsequent tsunami that caused a meltdown at the Fukushima Daiichi nuclear power plant on March 11th, 2011, modern nuclear safety protocols ensured zero instances of mortality and other direct human effects of radiation exposure. Follow-up studies however have shown concerns in terms of post-disaster recovery. More than 50,000 people still remain evacuated from the affected area. The stress of the evacuation can be directly linked to indirect casualties due to suicide, alcoholism, and other psychosocial consequences (Hasegawa, et al., 2015). Further, communities within decontaminated areas have low return rates and express difficulty in restarting economies (Yamane, et al., 2013). In general, the population of the Fukushima prefecture have shown poor resilience to the nuclear emergency. In response to this concern, supplementary work conducted during this master's degree study used lessons learnt in natural disaster management to investigate the use of social capital as a metric in developing initiatives to improve community resilience in the unlikely event of a nuclear emergency.

Social capital is a concept used to describe the use of relationships and interactions between individuals as a resource. While initially used in areas of sociology and political science, social capital has found useful applications in other fields. For example, when studying the disaster at Fukushima vast variations in mortality rates were identified between affected prefectures (National Police Agency of Japan, 2016). In analyzing this variation, political connections and the depth of social ties, strong indicators of social capital, showed greater influence on the rate of death than demographic factors or the height of local tsunami walls (Aldrich & Sawada, 2015). This is reflected in post-disaster research that has shown that in general, communities with greater resilience, returning to normal with fewer external resources, almost always use relationships, connections, and interactions between individuals of the community as a resource for recovery.

To bring this concept to the context of nuclear safety, preliminary research was conducted employing social capital as a metric to evaluate communities surrounding nuclear facilities. It was hoped results would give insight to resources that exist, as well as areas for investment and improvement to help the nuclear facility better serve their community. The first study location chosen was the Durham Region surrounding the Pickering Nuclear Generating station. Being immediately west of the

metropolitan city of Toronto, the population surrounding the nuclear facility has grown considerably to more than 211,448 (The Regional Municipality of Durham, 2017). As it reaches the end of its commissioned life, future directions for the nuclear plant have been the center of debate. In the latest provincial election, all electoral ridings surrounding the facility voted in favor of the party vowing to keep the reactor open until 2024, deciding against parties offering immediate decommissioning (CBC News, 2018).

In the days leading up to the election, paper surveys containing 28 multiple choice questions were conducted in a door-to-door fashion in selected neighborhoods of the Durham Region. Questions of the survey closely followed guidelines of the Social Capital IQ developed by the World Bank, with the intention of quantifying 6 dimensions of social capital: groups and networks, trust and solidarity, collective actions and cooperation, information and communication, social cohesion and inclusion, and empowerment and political action (Grootaert, et al., 2004). Neighborhood boundaries were defined following official descriptions by the Regional Municipality of Durham to allow further correlation of responses with demographic information using census data. Due to the involvement of human participants in the collection of data, the survey tool was evaluated and approved by the McMaster Research Ethics Board.

While still in the early stages of analysis, preliminary results of the study have revealed interesting insights about the communities surveyed. For example, most residents found nuclear energy relatively safe, reflecting their recent vote. Further, the survey showed residents who found nuclear energy safe in general also showed greater trust in the regulation of local and national nuclear agencies, while reporting slightly less trust towards global agencies (Figure 9).

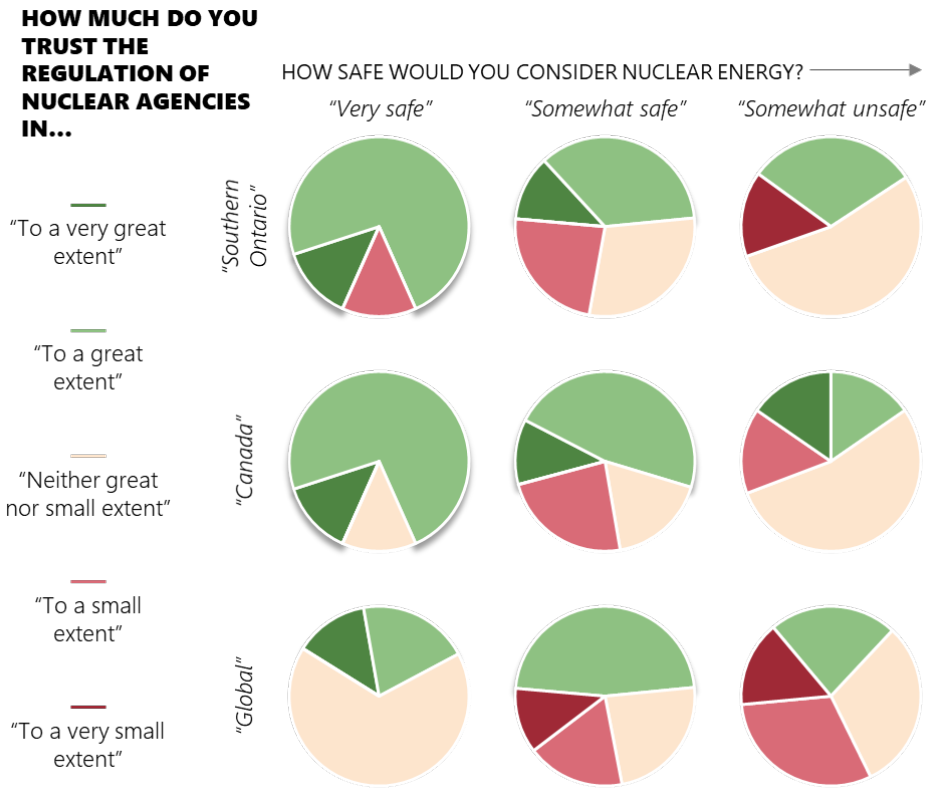

Figure 9 – Responses to the questions "How much do you trust the regulation of …?", as a function of "How safe would you consider nuclear energy?". Examples were given for each level: Southern Ontario – Ontario Power Generation, Canada – Canadian Nuclear Safety Commission, Global – International Atomic Energy Agency

Questions regarding social cohesion and inclusion, investigating inclusion, sociability, conflict and violence saw an almost even distribution in responses ranging from "very distant" to "very close" regarding the "feeling of togetherness or closeness in their neighborhood". Interestingly strong correlation was seen between how a resident responded regarding their 'feeling of closeness', and their belief on how compliant their neighborhood would be to evacuation instructions in the event of a nuclear emergency. As shown in Figure 10 Residents who felt very close to their neighbors believed they would be compliant "to a very great extent" while residents feeling more distant believed their neighbors would be compliant "to a very small extent".

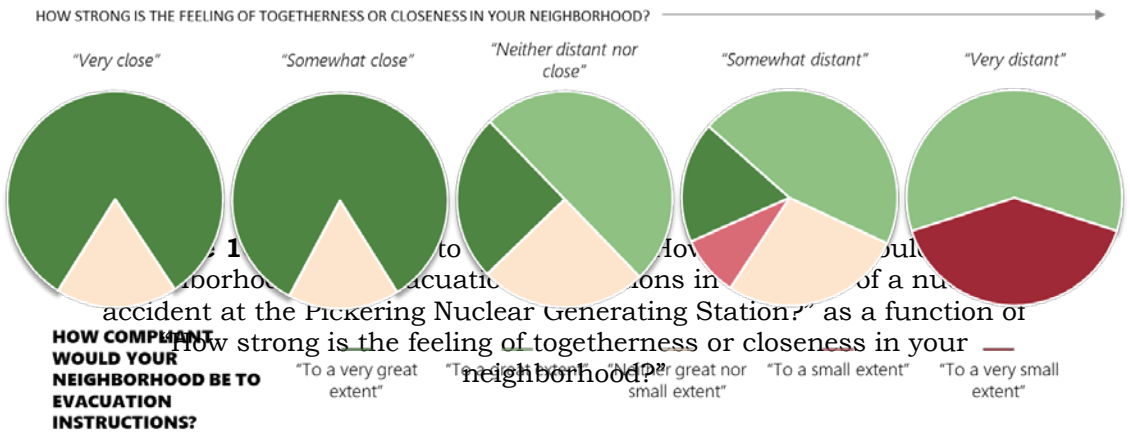

: 1 to ...ow ...ould ...borho... ...acuatic... ...ions in ...of a nu...
accident at the Pickering Nuclear Generating Station?" as a function of
"How strong is the feeling of togetherness or closeness in your neighborhood?"

Finally, as seen in Figure 11, survey results suggested a relationship between empowerment (the feeling of power one had to make important decisions that could change the course of their life), and the resident's belief of whether their neighborhood would come together to jointly petition or address a major concern regarding the Pickering Nuclear Generating Station.

Using social capital to quantify the effect of social phenomena allows for its effective use as a resource during decision making. This was seen in

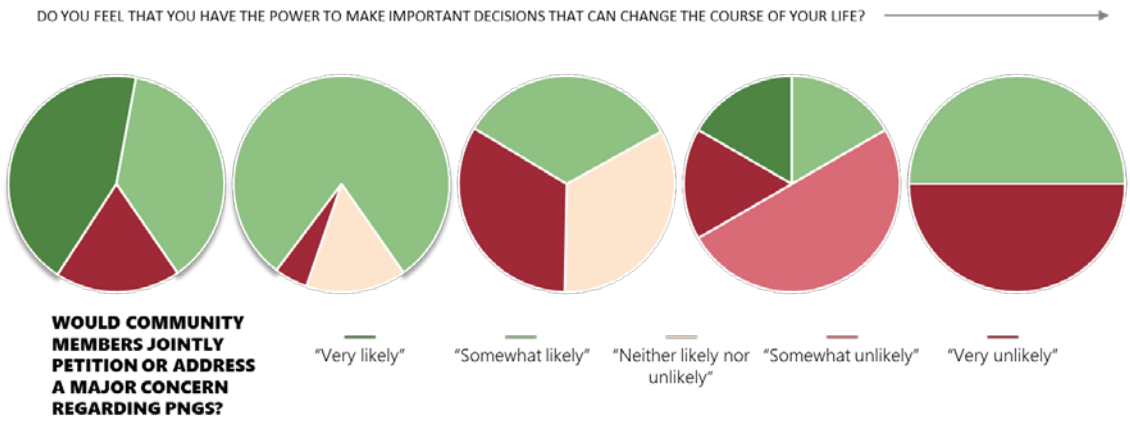

Figure 11 – Responses to the questions "If there were a major concern regarding the Pickering Nuclear Generating Station, how likely would it be for community members to get together to jointly petition or address the issue?" as a function of "Do you feel that you have the power to make important decisions that can change the course of your life?"

the study of community-based water projects in Central Java, Indonesia where social capital indicators did not return with positive associations to household health in the analysis of public wells but was a positive and significant determinant of improved household health in piped connections (Isham & Kähkönen, 2002). This was useful as it recognized, in context to

other resources involved in water projects, that investment in collective effort and cooperation was critical to the success of constructing and maintaining piped water systems.

Through further analysis of the interaction of responses to questions regarding multiple dimensions of social capital, it is hoped that actionable insights may be revealed regarding the studied communities surrounding the nuclear power plant. For example, following the observed relationship of trust described in Figure 9, further investigation may suggest residents in these communities would prefer and express greater compliance to a local, tailored evacuation order rather than a global response. This would also involve the analysis of demographic information and further available resources (including but not limited to economic resources) for each studied neighborhood provided by publicly available land survey and census data. For the case of the World Bank looking to answer questions regarding poverty reduction strategy, etc., the contribution from social capital to the household was compared in context to other assets available to the household, namely income, physical assets and other resources making consumption possible.

Moving forward, to truly resolve the under-representation of indirect consequences of exposure to radiation at doses relevant to nuclear incidents and accident, it is paramount that such effects be described

using a common metric. To be able to effectively communicate the detriment from low dose NTE at the cellular level – in comparable terms to detriment from consequences at the social level – in relation to currently well-defined metrics of detriment from direct effects of radiation, allows for a more holistic approach to nuclear safety. Such improvements to risk management and radiation protection of human and non-human biota would have meaningful impact to the adoption, and safe management of nuclear technologies and industrial applications.

REFERENCES

Aldrich, D. P. & Sawada, Y., 2015. The physical and social determinants of mortality in the 3.11 tsunami. *Social Science & Medicine,* January, Volume 124, pp. 66-75.

Aypar, U., Morgan, W. F. & Baulch, J. E., 2010. Radiation-induced genomic instability: Are epigenetic mechanisms the missing link?. *International Journal of Radiation Biology,* 87(2), pp. 179-191.

Batty, D. G. et al., 2017. Psychological distress in relation to site specific cancer mortality: pooling of unpublished data from 16 prospective cohort studies. *BMJ,* Volume 356.

Bishayee, A. et al., 2001. Free radical-initiated and gap junction-mediated bystander effect due to nonuniform distribution of incorporated radioactivity in a three-dimensional tissue culture model. *Radiat Res,* 155(2), pp. 335-344.

Blöcher, D., 1988. DNA Double-strand Break Repair Determines the RBE of α-particles. *International Journal of Radiation Biology,* June, 54(5), pp. 761-771.

Boice, J. D., 2017. The linear nonthreshold (LNT) model as used in radiation protection: an NCRP update. *International Journal of Radiation Biology,* 93(10), pp. 1079-1092.

Boukamp, P. et al., 1988. Normal keratinization in a spontaneously immortalized aneuploid human keratinocyte cell line.. *Journal of Cell Biology,* 1 March, 106(3), pp. 761-771.

Bréchignac, F., 2002. Environment versus man radioprotection: The need for new conceptual approach?. *Radioprotection,* Volume 37, pp. C1-161.

Brint, E. K. et al., 2004. ST2 is an inhibitor of interleukin 1 receptor and Toll-like receptor 4 signaling and maintains endotoxin tolerance. *Nature Immunology,* Volume 5, pp. 373-379.

Brunner, M. et al., 2004. Increased levels of soluble ST2 protein and IgG1 production in patients with sepsis and trauma. *Intensive Care Medicine,* Volume 30, pp. 1468-1473.

Burtt, J. J., Thompson, P. A. & Lafrenie, R. M., 2016. Non-targeted effects and radiation-induced carcinogenesis: a review. *J. Radiol. Prot,* Volume 36, pp. R23-R35.

Cairns, J., 2006. Cancer and the Immortal Strand Hypothesis. *Genetics,* 174(3), pp. 1069-1072.

CBC News, 2018. Doug Ford promises to keep Pickering nuclear plant open until 2024. *CBC News*, 21 June.

Chen, T.-M., Pecoraro, G. & Defendi, V., 1993. Genetic analysis of in vitro progression of human papillomavirus-transfected human cervical cells.. *Cancer Research,* 53(5), pp. 1167-1171.

Colotta, F. et al., 2009. Cancer-related inflammation, the seventh hallmark of cancer: links to genetic instability. *Carcinogenesis,* 30(7), pp. 1073-1081.

Ding, L.-H.et al., 2005. Gene Expression Profiles of Normal Human Fibroblasts after Exposure to Ionizing Radiation: A Comparative Study of Low and High Doses. *Radiation Research,* 164(1), pp. 17-26.

Eckert & Ziegler, 2010. *Recommended Nuclear Decay Data: Ra-226,* Braunschweig : Nuclitec GmbH.

Elkind, M. M., 1984. Repair Processes in Radiation Biology. *Radiation Research,* 100(3), pp. 425-449.

Fernandez-Palomo, C., Seymour, C. & Mothersill, C., 2016. Inter-Relationship between Low-Dose Hyper-Radiosensitivity and Radiation-Induced Bystander Effects in the Human T98G Glioma and the Epithelial HaCaT Cell Line. *Radiation Research,* Volume 185, pp. 124-133.

Fernet, M., Mégnin-Chanet, F., Hall, J. & Favaudon, V., 2010. Control of the G2/M checkpoints after exposure to low doses of ionising radiation: Implications for hyper-radiosensitivity. *DNA Repair,* 9(1), pp. 48-57.

Gold, B., 2017. Somatic mutations in cancer: Stochastic versus predictable. *Mutation Research/Genetic Toxicology and Environmental Mutagenesis,* Volume 814, pp. 37-46.

Goodhead, D. T., 1994. Initial events in the cellular effects of ionizing radiations: clustered damage in DNA. *Int. J. Radiat. Biol.,* November, 65(1), pp. 7-17.

Grootaert, C., Narayan, D., Jones, V. N. & Woolcock, M., 2004. *Measuring Social Capital: An Integrated Questionnaire,* Washington, D.C.: The World Bank.

Haga, Y. et al., 2003. The effect of ST2 gene product on anchorage-independent growth of a glioblastoma cell line, T98G. *European Journal of Biochemistry,* 270(1), pp. 163-170.

Hall, E. J. & Giaccia, A. J., 2006. *Radiobiology for the radiologist.* 6th ed. Philadelphia(PA): Lippincott WIlliams & Wilkins.

Hasegawa, A. et al., 2015. Health effects of radiation and other health problems in the aftermath of nuclear accidents, with an emphasis on Fukushima. *The Lancet,* 386(9992), pp. 479-488.

Higley, K. A., Kocher, D. C., Real, A. G. & Chambers, D. B., 2012. Relative biological effectiveness and radiation weighting factors in the context of

animals and plants. *Annals of the ICRP,* October-December, 41(3-4), pp. 233-243.

IAEA, 2013. *INES: The International Nuclear and Radiological Event Scale User's Manual - 2008 Edition,* Vienna: Co-sponsered by the IAEA and OECD/NEA.

ICRP, 2007. *The 2007 Recommendations of the International Commission on Radiological Protection. ICRP Publication 103 Ann. ICRP 37 (2-4),* s.l.: Elsevier Ltd for International Commission on Radiological Protection.

Ilnytskyy, Y., Koturbash, I. & Kovalchuk, O., 2009. Radiation-Induced Bystander Effects In Vivo are Epigenetically Regulated in a Tissue-Specific Manner. *Environmental and Molecular Mutagenesis,* Volume 50, pp. 105-113.

Isham, J. & Kähkönen, S., 2002. How Do Participation and Social Capital Affect Community-Based Water Projects? Evidence from Central Java, Indonesia. In: *The Role of Social Capital in Development.* New York: Cambridge University Press, pp. 155-187.

Joiner, M. C. et al., 2001. Low-dose hypersensitivity: current status and possible mechanisms. *International Journal of Radiation Oncology*Biology*Physics,* 49(2), pp. 379-389.

Kadhim, M. A. et al., 1994. (Alpha)-particle-induced chromosomal instability in human bone marrow cells. *The Lancet,* 344(8928), pp. 987-988.

Kadhim, M. A. et al., 1992. Transmission of chromosomal instability after plutonium α-particle irradiation. *Nature,* Volume 355, pp. 738-740.

Kadhim, M. et al., 2013. Non-targeted effects of ionising radiation-Implications for low dose risk. *Mutation Research,* 752(2), pp. 84-98.

Katsarska, O. et al., 2016. The soluble receptor ST2 is positively associated with occupational exposure to radiation. *International Journal of Radiation Biology,* 92(2), pp. 87-93.

Lambin, P. et al., 1993. Hypersensitivity of a human tumour cell line to very low radiation doses.. *Int J Radiat Biol,* May, Volume 63, pp. 639-50.

Limoli, C. L. et al., 2000. Genomic instability induced by high and low LET ionizing radiation. *Adv. Space Res.,* 25(10), pp. 2107-2117.

Little, M. P. & Hendry, J. H., 2017. Mathematical models of tissue stem and transit target cell divisions and the risk of radiation- or smoking-associated cancer. *PLOS Computational Biology.*

Little, M. P., Hendry, J. H. & Puskin, J. S., 2016. Lack of Correlation between Stem-Cell Proliferation and Radiation- or Smoking-Associated Cancer Risk. *PLOS ONE.*

Lorimore, S. A., Coates, P. J. & Wright, E. G., 2003. Radiation-induced genomic instability and bystander effects: inter-related nontargeted effects of exposure to ionizing radiation. *Oncogene,* Volume 22, pp. 7058-7069.

Lyng, F. M. et al., 1996. Persistent expression of morphological abnormalities in the distant progeny of irradiated cells. *Radiat Environ Biophys,* October, 35(4), pp. 273-283.

Marcus, P. I., Cieciura, S. J. & Puck, T. T., 1956. CLonal growth in vitro of epithelial cells from normal human tissues. *JEM,* 104(4), pp. 615-628.

Marples, B., Lambin, P., Skov, K. A. & Joiner, M. C., 1997. Low dose hyper-radiosensitivity and increased radioresistance in mammalian cells. *Int. J. Radiat. Biol,* 71(6), pp. 721-735.

Miller, R. C. et al., 1999. The oncogenic transforming potential of the passage of single α particles through mammalian cell nuclei. *PNAS,* January, 96(1), pp. 19-22.

Morgan, W. F., 2003. Non-Targeted and Delayed Effects of Exposure to Ionizing Radiation: II. Radiation-Induced Genomic Instability and Bystander Effects In Vivo, Clastogenic Factors and Transgenerational Effects. *Radiation Research,* 159(5), pp. 581-596.

Morgan, W. F. et al., 1996. Genomic Instability Induced by Ionizing Radiation. *Radiation Research,* 146(3), pp. 247-258.

Mori, S. et al., 2009. An Anchorage-Independent Cell Growth Signature Identifies Tumors with Metastatic Potential. *Oncogene,* 6 August, 28(31), pp. 2796-2805.

Mothersill, C. et al., 2000. Dose- and time-response relationships for lethal mutations and chromosomal instability induced by ionizing radiation in an immortalized human keratinocyte cell line. *International Journal of Radiation Biology,* 76(6), pp. 799-806.

Mothersill, C. & Seymour, C., 2012. Changing paradigms in radiobiology. *Mutation Research,* April, 750(2), pp. 85-95.

Mothersill, C. & Seymour, C., 2018. Old data - new concepts: integrating "indirect effects" into radiation protection. *Health Phys.,* 115(1), pp. 170-178.

Mothersill, C., Seymour, C. B. & Joiner, M. C., 2002. Relationship between Radiation-Induced Low-Dose Hypersensitivity and the Bystander Effect. *Radiation Research,* 157(5), pp. 526-532.

Nagasawa, H. & Little, J. B., 1999. Unexpected Sensitivity to the Induction of Mutations by Very Low Doses of Alpha-Particle Radiation: Evidence for a Bystander Effect.. *Radiation Research,* November, 152(5), pp. 552-557.

National Police Agency of Japan, 2016. *Damage Situation and Police Countermeasures associated with 2011 Tohoku district - off the Pacific Ocean Earthquake,* s.l.: s.n.

Noble, R., Kaltz, O. & Hochberg, M. E., 2015. Peto's paradox and human cancers. *Philos Trans R Soc Lond B Biol Sci,* 370(1673).

Noble, R., Kaltz, O., Nunney, L. & Hochberg, M. E., 2016. Overestimating the Role of Environment in Cancers. *Cancer Prevention Research,* 9(10), pp. 773-776.

Pierce, D. A. & Preston, D. L., 2000. Radiation-Related Cancer Risks at Low Doses among Atomic Bomb Survivors. *Radiation Research,* Volume 154, pp. 178-186.

Quesenberry, P. J. & Goldberg, L. R., 2015. Stem cell divisions and cancer. *Leukemia,* Volume 29, p. 1959.

R Development Core Team, 2008. *R: A Language and Environment for Statistical Computing.* Vienna: R Foundation for Statistical Computing.

Ryan, L. A., Seymour, C. B., Joiner, M. C. & Mothersill, C. E., 2009. Radiation-induced adaptive response is not seen in cell lines showing a bystander effect but is seen in lines showing HRS/IRR response. *International Journal of Radiation Biology,* 85(1), pp. 87-95.

Ryan, L. A., Seymour, C. B., Neill-Mehlenbacher, A. O. & Mothersill, C. E., 2008. Radiation-induced adaptive response in fish cell lines. *Journal of Environmental Radioactivity,* October, Volume 99, pp. 739-747.

Schoenherr, D. et al., 2013. Determining if low dose hyper-radiosensitivity (HRS) can be exploited to provide a therapeutic advantage: A cell line study in four glioblastoma multiforme (GBM) cell lines. *International Journal of Radiation Biology,* 89(12), pp. 1009-1016.

Scott, B. R. et al., 2003. Mechanistic Basis for Nonlinear Dose-Response Relationships for Low-Dose Radiation-Induced Stochastic Effects. *Nonlinearity Biology Toxicol Med,* 1(1), pp. 93-122.

Seymour, C. B. & Mothersill, C., 2000. Relative Contribution of Bystander and Targeted Cell Killing to the Low-Dose Region of the Radiation Dose-Response Curve. *Radiation Research,* 153(5), pp. 508-511.

Seymour, C., Mothersill, C. & Alper, T., 1986. High Yields of Lethal Mutations in Somatic Mammalian Cells that Survive Ionizing Radiation. *International Journal of Radiation Biology and Related Studies in Physics, Chemistry and Medicine,* 50(1), pp. 167-179.

Shi, X., 2016. *Study of bioaccumulation and radiobiological effects of environmentally relevant level of radium-226,* Hamilton: McMaster University.

Short, S. et al., 1999. Low dose hypersensitivity in the T98G human glioblastoma cell line. *International Journal of Radiation Biology,* 75(7), pp. 847-855.

Smith, L. E., Nagar, S., Kim, G. J. & Morgan, W. F., 2003. Radiation-induced genomic instability: radiation quality and dose response. *Health Phys,* 85(1), pp. 23-29.

Stein, G. H., 1979. T98G: An anchorage-independent human tumor cell line that exhibits stationary phase G1 arrest in vitro. *Journal of Cellular Physiology,* April, 99(1), pp. 43-54.

The Regional Municipality of Durham, 2017. *2016 Census of Population - Population and Dwelling Counts Release, File: D01-03, Table 1a,* Pickering: Commissioner of Planning and Economic Development.

Thomas, P. et al., 2007. Relative biological effectiveness (RBE) of alpha radiation in cultured porcine aortic endothelial cells. *International Journal of Radiation Biology,* 83(3), pp. 171-179.

Tomasetti, C. & Vogelstein, B., 2015. Variation in cancer risk among tissues can be explained by the number of stem cell divisions. *Science,* 347(6217), pp. 78-81.

Weissenborn, U. & Streffer, C., 1988. Analysis of Structural and Numerical Chromosomal Anomalies at the First, Second, and Third Mitosis after

Irradiation of One-cell Mouse Embryos with X-rays or Neutrons. *International Journal of Radiation Biology,* 54(3), pp. 381-394.

Weissenborn, U. & Streffer, C., 1989. Analysis of Structural and Numerical Chromosomal Aberrations at the First and Second Mitosis after X Irradiation of Two-Cell Mouse Embryos. *Radiation Research,* Volume 117, pp. 214-220.

Wrixon, A. D., 2008. New ICRP recommendations. *J. Radiol. Prot,* 22 May, 28(2), pp. 161-168.

Wu, S., Powers, S., Zhu, W. & Hannun, Y. A., 2016. Substantial contribution of extrinsic risk factors to cancer development. *Nature,* Volume 529, pp. 43-47.

Yamane, F., Ohgaki, H. & Asano, K., 2013. The Immediate Impact of the Fukushima Daiichi Accident on Local Property Values. *Risk Analysis,* 33(11), pp. 2023-2040.